Landau theory of phase transitions in TTF-TCNQ

C. Hartzstein, V. Zevin, M. Weger

▶ To cite this version:

C. Hartzstein, V. Zevin, M. Weger. Landau theory of phase transitions in TTF-TCNQ. Journal de Physique, 1980, 41 (7), pp.677-699. 10.1051/jphys:01980004107067700 . jpa-00209294

HAL Id: jpa-00209294

https://hal.science/jpa-00209294

Submitted on 4 Feb 2008

HAL is a multi-disciplinary open access archive for the deposit and dissemination of scientific research documents, whether they are published or not. The documents may come from teaching and research institutions in France or abroad, or from public or private research centers.

L'archive ouverte pluridisciplinaire **HAL**, est destinée au dépôt et à la diffusion de documents scientifiques de niveau recherche, publiés ou non, émanant des établissements d'enseignement et de recherche français ou étrangers, des laboratoires publics ou privés.

Classification
Physics Abstracts
61.65 — 63.20K — 64.70K — 65.40

Landau theory of phase transitions in TTF-TCNQ

C. Hartzstein, V. Zevin and M. Weger

Racah Institute of Physics, The Hebrew University, Jerusalem, Israel

(*Reçu le 2 mai 1979, révisé le 16 janvier, accepté le 13 mars 1980*)

Résumé. — On calcule plusieurs paramètres de l'énergie libre de Landau pour TTF-TCNQ à partir de la structure cristalline en tenant compte de la position des atomes et des distributions de charge réalistes. En particulier, on évalue les paramètres qui déterminent le couplage entre les ondes de densité de charge et les rotations (*librons*) sur des chaînes voisines. On résoud la fonction d'énergie libre et on obtient un bon accord avec l'observation expérimentale de la période 2 a entre 53 K et 48 K et sa variation en dessous de cette température. L'interaction « onde de densité de charge »-libron semble être responsable pour cette période transversale. On étudie le comportement de C_p aux environs des deux transitions de phases voisines. L'énergie libre devrait avoir plusieurs (jusqu'à quatre) points de Lifshitz, pour des valeurs convenables des paramètres.

Abstract. — Several parameters of the Landau Free Energy Function of TTF-TCNQ are calculated from the crystal structure taking into account the atomic positions and realistic charge distributions. In particular, the parameters that determine the coupling between charge density waves and rotations (*librons*) on neighbouring chains are evaluated. The Free Energy Function is solved, and good agreement with the experimental observation of the 2 a period between 53 K and 48 K and its variation below this temperature, is obtained. The CDW-libron interaction seems to be responsible for this transverse period. The behaviour of C_p in the vicinity of the two close phase transitions is studied. The Free Energy should possess several (up to four) Lifshitz points, for appropriate values of the parameters.

1. **Introduction.** — It is known that the organic charge-transfer metal TTF-TCNQ (tetrathiofulvalene tetracyanoquinodimethanide) undergoes a cascade of three nearby phase transitions [1-10]. The first two are second order and occur at the transition temperatures $T_{p1} = 53$ K and $T_{p2} = 48$ K, the third is a first order phase transition and occurs at 38 K. It is believed that the two first transitions can be made to coincide by changing the stoichiometric coefficients in

$$\mathrm{TTF}_{(1-x)}\mathrm{TSeF}_x\mathrm{TCNQ}\,.$$

In TSeF-TCNQ both transitions apparently coincide at 29 K [11].

In TTF-TCNQ, a charge density wave (CDW) builds up at T_{p1} with a longitudinal period of $\Lambda = 3.39\,b$ and a transverse period of $2\,a$. At T_{p2} a second CDW appears and the transverse period begins to increase continuously. At the temperature of 38 K, TTF-TCNQ undergoes the third phase transition, where the transverse period jumps to the commensurate value $4\,a$ [12].

In this study we discuss only the phase-diagram and other features which are connected with the two nearby higher temperature phase transitions.

The Landau theory of the phase transitions was applied to TTF-TCNQ first by Bak and Emery [13], Schultz and Etemad [14], Bjelis and Barisic [15] and more recently by several authors [16, 17, 18, 19]. These authors make use of the symmetry properties of the lattice, and derive those properties that are an essential consequence of this symmetry; namely, the existence of two transition temperatures, T_{p1} and T_{p2}, and the change in the transverse period only below T_{p2}. However, the amount of information that can be derived from symmetry alone is limited. For example, TSeF-TCNQ which has the same symmetry as TTF-TCNQ, has only one phase transition, and application of small pressure to TTF-TCNQ, which does not change the lattice symmetry, has a drastic effect on the phase diagram. Therefore, symmetry properties alone are not sufficient to give a complete description of these complicated systems, and numerical calculations of the various parameters in the LFEF are necessary. A first step in that direction was made in a previous paper [21] where some of the parameters were estimated from the lattice structure, and the importance of the librational degrees of freedom, already introduced by Morawitz [20], was stressed.

Weger and Friedel [21] showed that the CDW-Libron interaction between nearest chains in the a^*-direction should provide the main contribution to the

Article published online by EDP Sciences and available at http://dx.doi.org/10.1051/jphys:01980004107067700

effective interaction between nearest similar chains; especially when it is realized that the direct Coulomb interaction (DCI) between nearest similar chains should be screened by the interposing chains of the other type.

In ref. [21], 4 order parameters were employed; ρ_Q and χ_Q for the TCNQ's, and ρ_F and χ_F for the TTF's. The $\rho_Q(\rho_F)$ parameter describes a distortion which has the symmetry of a longitudinal phonon, namely symmetry group P2/m for an isolated TCNQ(TTF) chain; the $\chi_Q(\chi_F)$ parameter describes a distortion with the symmetry of a libration in the molecular plane, or around the long molecular axis, namely symmetry group P2/*b* for an isolated TCNQ(TTF) chain.

When we have a LFEF with a given number of order parameters : $F(x_1 \dots x_n)$, we can *always* reduce the number of order parameters by algebraic elimination; i.e. solve the equations :

$$\frac{\partial F}{\partial x_i} = 0 \ (i = 1, \dots, m)$$

and derive from them the x_i's ($i = 1, \dots, m$) as function of the x_j's ($j = m + 1, \dots, n$), put the values of the x_i back into F, and thus obtain a function $F(x_{m+1}, \dots, x_n)$ with less variables.

In the present case, we can, for example, eliminate the order parameters χ_Q and χ_F, and be left with a function $F(\rho_Q, \rho_F)$ which appears to be equivalent to the function used by several authors [13, 14, 15, 16]. If we wish we can go further and eliminate ρ_F, obtaining a function $F(\rho_Q)$, or even further, and eliminate ρ_Q, obtaining just a number F.

The question here is not whether such an elimination is mathematically correct, but whether it is useful and fruitful. When we perform a partial elimination we obtain a function of less variables, which looks at first sight simpler. However, we also lose in the process.

First, the coefficients of the *bare* LFEF can be calculated (or at least estimated) from first principles. We calculate a few parameters in this work. In contrast, the coefficients of the reduced LFEF must be fitted to experiment, and be regarded as no more than a representation of experimental results, or, alternatively, be calculated from the coefficients of the *bare* LFEF as we do here. Thus, for any linkage with an *ab-initio* calculation, the *bare* coefficients are essential.

Second, the coefficients of the reduced LFEF become complicated functions of temperature, pressure, and the other variables. They may even be non-analytic functions. The coefficients of the *bare* LFEF are much more nearly constant. Thus, if we try to take into account the complicated temperature, pressure, etc., dependence of these coefficients, say by some power series expansion, we actually end up with *more* adjustable parameters than there are in the *bare* LFEF, and the description is much more complicated.

Third, the order parameters of the *bare* LFEF are very simply related to measurable quantities such as molecular translations and rotations, phonon frequencies [22], etc. Thus we can make use of available experimental data, and we can make predictions that could not be made from the reduced LFEF. For example the detailed theory of the conductivity in the metallic state [23] is a direct outcome from the *bare* LFEF, which demonstrated the importance of the libron degree of freedom.

Because of the very large number of order parameters, the LFEF contains, in principle, a very large number of terms. Even if only nearest neighbour chain interactions within the *a-b* plane are included (Fig. 1), and only one type of translation and one type of rotation in each chain are considered, there are about 50 terms up to the 4th order. Therefore, by appropriate choice of the parameters, just about any result can be obtained. In order that the results be meaningful, the parameters in the LFEF must be estimated from *ab-initio* considerations (i.e. the crystal structure, the various microscopic constants, etc.) rather than arbitrarily fitted by experiment. Of course, it is a very hard task to fulfill such a program for as complicated a system as TTF-TCNQ in a rigorous way. Here we limit ourselves to the monopole-monopole electrostatic interactions and the simple mean field (MF) approach as the first step to more comprehensive *ab-initio* calculations.

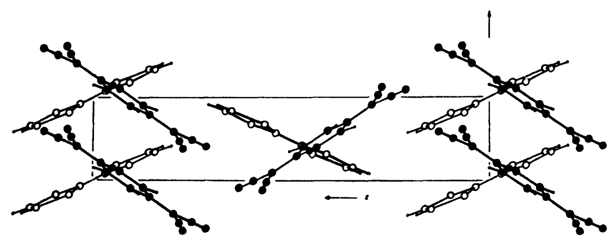

a)

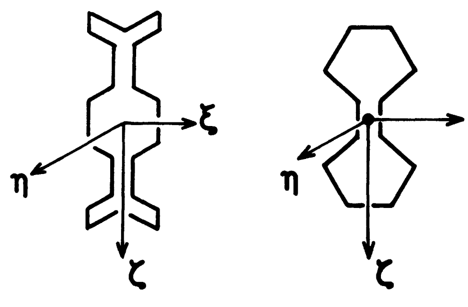

b)

Fig. 1. — *a*) A view of the crystal packing in TTF-TCNQ. The shaded molecules have their centroids at $x = a/2$ (from Kistenmacher *et al.* [56]). *b*) Definition of the molecular axes.

In our preliminary short report [24] we used the CDW-libron interaction model of Weger and Friedel [21] in which the extra charge of the

$$\mathrm{TCNQ}^{-0.6}\ (\mathrm{TTF}^{+0.6})$$

molecule was located only on the nitrogens (the sulphur and end carbon) atoms. In this paper we also use another model with the more realistic picture of the charge distribution, based on the charge distribution calculations of Ladik *et al.* [25] for the TCNQ, $TCNQ^-$, TTF^+ and TTF molecules. The two models are compared in section 5 and the importance of the intramolecular screening for the case of the second model is discussed.

The paper is organized as follows :

In section 2 we discuss the elementary solutions of the LFEF and show the temperature dependence of the order parameters, the transverse period and the heat capacity for various sets of the LFEF interaction parameters.

In section 3, we estimate the value of the LFEF parameters for the CDW-libron [21] model and the direct Coulomb interaction parameters are considered in section 4. In section 5 the values of the parameters used in the numerical calculations are compared with the estimates of the preceding sections. The validity of these estimates is discussed. In section 6 we show that two (or four) Lifshitz points [26] may appear on the phase diagram of the TTF-TCNQ system and discuss some features of this phase diagram. Details of the calculations are presented in Appendices I and II.

It is worthwhile to note that TTF-TCNQ is one of the several systems in which phase transitions occur at very nearby temperatures. For example, in V_3Si, a displacive phase transitions occurs at $T_M = 22$ K and a superconducting one at $T_c = 17$ K [27]. Under pressure, T_M and T_c approach until they coincide at about 35 kbar [28, 29]. T_M is, strictly speaking, a first order transition, however, its latent heat is very small, and it is close to a second-order one.

In dichalcogenides, like $NbSe_2$, a CDW builds up at a $T_p = 26$ K and superconductivity at $T_c = 7$ K, under pressure, T_p and T_c can be made to coincide [30]. In all these systems, we deal with two order parameters which are weakly coupled. In the two above-mentioned cases, this is because they characterize different physical properties. The closeness of the two transition temperatures may either be accidental (due to appropriate choice of external parameters-like pressure, for instance), or due to some complicated physical reason, such as the degeneracy of T_p and T_c in quasi-1d-systems suggested by Bychkov *et al.* [31]. The closeness of the two phase-transitions T_{p1} and T_{p2} in TTF-TCNQ and their interdependence is discussed here.

2. **Elementary solution of the free energy function.** — In this section we discuss the general picture of the phase transitions in TTF-TCNQ as it follows from the solutions of the LFEF suggested by Weger and Friedel [21] and completed here with the nearest similar chains DCI.

The simplified LFEF has the form :

$$\begin{aligned} F = {} & A_{11}(T)\,\rho_Q^2 + C_{11}\,\rho_Q^4 + A_{22}(T)\,\rho_F^2 + C_{22}\,\rho_F^4 \\ & + A_{33}\,\chi_Q^2 + A_{44}\,\chi_F^2 - 2\,A_{12}\,u \\ & - \rho_Q\,\rho_F - 2\,A_{14}\sqrt{(1-u^2)}\,\rho_Q\,\chi_F \\ & - 2\,A_{23}\sqrt{(1-u^2)}\,\rho_F\,\chi_Q \\ & - A_{11}[a]\,(1-2\,u^2)\,\rho_Q^2 - A_{22}[a]\,(1-2\,u^2)\,\rho_F^2 \end{aligned} \tag{1}$$

where the indices 1, 2, 3 and 4 correspond to the order parameters ρ_Q, ρ_F, χ_Q and χ_F respectively ;

$$u = \cos\frac{q_a\,a}{2}$$

where q_a is the wave number in the a direction transverse to the stack direction. A_{12} is the CDW-CDW coupling parameter between nearest chains, A_{14} and A_{23} are the coupling parameters of the CDW-libron interaction for nearest chains and $A_{11}[a]$ and $A_{22}[a]$ are the direct coupling parameters for nearest similar TCNQ and TTF chains respectively. The LFEF represents a two-dimensional model of quasi one dimensional conductors composed of weakly coupled chains. The order parameters fields are of the form

$$\eta_i(x, y) = \eta_i \exp[i(2\,\pi y/\Lambda + q_a\,x + \varphi_i)]\,, \qquad i = 1, 2, 3, 4.$$

The interactions in the c^*-direction are neglected [21]. We do not include in eq. (1) the libron-libron interaction term ($\propto A_{34}\,\chi_Q\,\chi_F$). Several fourth order terms are also neglected.

The second order phase transitions found in TTF-TCNQ are of the Peierls type [32-34] whose order parameter may be defined in several ways. It may be defined as the gap in the one-electron spectrum ; it may be defined as the amplitude of the charge density wave, i.e., the variation in the charge of the molecules ; or, it may be defined as some specific displacement of the molecules. All these definitions are equivalent, however, in order to assign well-defined numerical values to the parameters of the LFEF, we have to agree on some convention. In the present work, we define the order parameters ρ_Q and ρ_F as the molecular centre of gravity displacement in the b-direction in units of 1/100 Å. Some of the condensation energy of the Peierls transition is due to coupling with intramolecular modes, such as CN, CC, and CS stretching modes [35]. However, we still do not know the relative contribution of these modes to the condensation energy. Also, transverse phonons polarized in the c^*-direction, are coupled strongly to the Peierls distortion, in addition to longitudinal ones [36] (polarized in the b-direction). In an *ab-initio* calculation of the Peierls transition temperature, all these modes must be taken into account. However, here we use the experimental value of T_{pi}, $i = 1, 2$ and estimate from it the effective electron phonon coupling constant λ. Therefore, we express the order parameter of the Peierls transition in terms of one mode only — say the longitudinal phonon — since this is the mode that (probably) couples most strongly with the conduction electrons. The actual amplitude of displacement should not be too different (within a factor of 2 or 3) from that calculated on the basis of exclusive coupling with this mode. Since the definition of the order parameter is a matter of convention, the value of the free energy, its derivatives (i.e. specific heat), etc., will not depend on this choice.

Weger and Friedel [21] pointed out that the η-librations (i.e. librations in the molecular plane) are most effective — from the geometrical point of view — in producing the N-S and the N-C distance modulation, but we show in section 3 that for TCNQ molecules the ζ-libration (i.e. a libration around the long molecular axis) (see Fig. 1*b*) must also be taken into account. Therefore in this paper χ_F is a pure η-type libration and χ_Q is a linear combination of η and ζ librations, as defined in section 3.

To establish the appropriate phase diagram for our system, we use here the usual mean field approach and neglect the temperature dependence of all the coefficients in eq. (1) except for $A_{11}(T)$ and $A_{22}(T)$. (See, however, the discussion concerning the temperature dependence of the A_{14} and A_{23} parameters in section 3 and section 5.) For these two coefficients we assume that in the vicinity of the unrenormalized Peierls transition temperature T_i $(i = 1, 2)$ of the uncoupled chains

$$A_{ii} = \alpha_{ii}(T - T_i)/T_i . \tag{2}$$

We use the minimum conditions

$$\frac{\partial F}{\partial \eta_i} = 0, \quad i = 1, 2, 3, 4 , \quad \text{and} \quad \frac{\partial F}{\partial u} = 0 \tag{3}$$

to find the transition temperatures T_{p1} and T_{p2} of the weakly interacting subsystems $(\rho_Q\, \chi_F)$ and $(\rho_F\, \chi_Q)$ into which the LFEF naturally divides when $A_{12} = 0$, and the temperature dependence of the order parameters $\eta_i = \eta_i(T)$ and of the transverse period $u = u(T)$.

The solution of eq. (3) gives the following connection between the order parameters and the parameter u

$$\chi_F^2 = (A_{14}/A_{44})^2\, \rho_Q^2(1 - u^2) \tag{4a}$$

$$\chi_Q^2 = (A_{23}/A_{33})^2\, \rho_F^2(1 - u^2) \tag{4b}$$

$$u = A_{12}\, \rho_Q\, \rho_F/[(A_{14}^2/A_{44} + 2\, A_{11}[a])\, \rho_Q^2 + (A_{23}^2/A_{33} + 2\, A_{22}[a])\, \rho_F^2] , \quad u < 1 . \tag{4c}$$

Using eq. (4*a*) and eq. (4*b*) the libration order parameters may be eliminated from eq. (1) and eq. (1) may be cast in the form

$$\begin{aligned} F_{\text{eff}} = {} & [A_{11}(T) - A_{11}[a] - A_{14}^2/A_{44}]\, \rho_Q^2 + \\ & + [A_{22}(T) - A_{22}[a] - A_{23}^2/A_{33}]\, \rho_F^2 \\ & - 2\, A_{12}\, u\rho_Q\, \rho_F + [2\, A_{11}[a] + A_{14}^2/A_{33}]\, u^2\, \rho_Q^2 \\ & + [2\, A_{22}[a] + A_{23}^2/A_{44}]\, u^2\, \rho_F^2 + C_{11}\, \rho_Q^4 + C_{22}\, \rho_F^4 \end{aligned} \tag{1a}$$

which is valid when the conditions

$$\frac{\partial F}{\partial \chi_F} = \frac{\partial F}{\partial \chi_Q} = 0$$

are fulfilled (with $\partial^2 F/\partial \chi_F^2$, $\partial^2 F/\partial \chi_Q^2 > 0$). Eq. (1*a*) has the same form as the equation used, for instance, by Bjelis and Barisic [15]. Thus, their formulae for the phase temperature renormalization and for the phase transition lines (see eqs. (6)-(10) in ref. [15]) apply also here with the following correspondence between the parameters of LFEF

$$\left.\begin{matrix} A_{11}[a] \leftrightarrow \dfrac{A_{14}^2}{A_{44}} \leftrightarrow A_{11}[a] + \dfrac{A_{14}^2}{A_{44}} \\ A_{22}[a] \leftrightarrow \dfrac{A_{23}^2}{A_{33}} \leftrightarrow A_{22}[a] + \dfrac{A_{23}^2}{A_{33}} \end{matrix}\right\} \left\{\begin{matrix} \text{for the temperature} \\ \text{renormalization } \Delta T_1 \text{ and } \Delta T_2 \text{ (see eq. (8}a\text{) and eq. (8}b\text{))} \end{matrix}\right. \tag{5a}$$

$$\left.\begin{matrix} 2\, A_{11}[a] \leftrightarrow \dfrac{A_{14}^2}{A_{44}} \leftrightarrow 2\, A_{11}[a] + \dfrac{A_{14}^2}{A_{44}} \\ 2\, A_{22}[a] \leftrightarrow \dfrac{A_{23}^2}{A_{33}} \leftrightarrow 2\, A_{22}[a] + \dfrac{A_{23}^2}{A_{33}} \end{matrix}\right\} \left\{\begin{matrix} \text{for the } u^2 \text{ term} \\ \text{in eq. (4}c\text{)} \end{matrix}\right. \tag{5b}$$

Here the first column corresponds to the DCI between nearest similar chains only, the second — to the CDW-libron nearest different chains only and the third column corresponds to the case when both interactions are significant. Thus, we see that the CDW-libron interaction between the *nearest* chains provide an effective coupling between the *next-nearest* chains. The question arises : which coupling is dominant ?

We show further that if the screening effect somewhat diminishes the DCI terms $A_{11}[a]$ and $A_{22}[a]$ the only mechanism which is responsible for the transverse ordering in TTF-TCNQ is the CDW-libron interaction. In any case, the renormalization of the next nearest chains interaction due to the CDW-libron coupling is an important factor in building up the transverse period (see section 5).

The neglect of the interaction between the CDW in one type of chains with *transverse* phonons in the chains of the *second* type was justified by Weger and Friedel (see Table I of reference [21]). Transverse phonons polarized in the x-direction do not couple with a CDW in the neighbouring chain for a quarter filled band (the interaction coefficient includes a factor $\cos(q_b b)$ that is zero for such a filling) and the coupling must be small for a 0.59 electron per atom filling. The opposite is true for the interaction between transverse phonons polarized in the z-direction with CDW in the neighbouring chains. Its interaction coefficient is proportional to $\sin(q_b b)$ which is maximum for a quarter filled band. Moreover, the corresponding term in the LFEF contains a factor $\cos(q_a a/2)$ instead of the $\sin(q_a a/2)$ appearing in the CDW-libron interaction terms. The former would lead to an « a » period instead of a « $2a$ » period in the 48 K-53 K temperature range. In order to fully justify the neglect of the transverse phonon (z-polarized)-CDW interaction we estimated its coefficient A_{1z} in the same way as we did with A_{14} and we obtained $A_{1z} = 0.011$ meV/$(10^{-2}$ Å$)^2$. The right comparison must be done between

$$A_{1z}^2/A_{zz} = 0.002\ \text{meV}/(10^{-2}\ \text{Å})^2$$

($A_{zz} = 0.062$ meV/$(10^{-2}$ Å$)^2$ is the force constant obtained from reference [55]) and (see Table VI)

$$A_{14}^2/A_{44} = 0.060\ \text{meV}/(10^{-2}\ \text{Å})^2 .$$

The former is 30 times smaller than the latter and its neglect is fully justified. This argument does not apply to coupling with the transverse phonon polarized in the c^*-direction on the *same* chain since this phonon has the same symmetry as the longitudinal one, the coupling is strong, as seen by the diffuse X-ray and neutron diffraction work.

For the sake of simplicity and because of the correspondence relation, eq. (5), in the following we shall use the second column of eq. (5) only.

From eq. (1*a*) and eq. (3) we obtain for the temperature range $T_{p2} \leqslant T \leqslant T_{p1}$

$$\rho_Q^2 = \frac{\alpha_{11}}{2\,C_{11}}\,\frac{(T_{p1} - T)}{T_1} \tag{6a}$$

$$\rho_F = 0\,,\quad \chi_Q = 0\,,\quad u = 0\,. \tag{6b}$$

For the temperature range $T \lesssim T_{p2} < T_{p1}$ we obtain

$$\rho_F^2 \simeq \frac{\alpha_{22}}{2(C_{22} + \Delta C_{22})}\,\frac{(T_{p2} - T)}{T_2} \tag{7a}$$

$$\Delta C_{22} = A_{12}^2\,\frac{(A_{23}^2/A_{33})}{(A_{14}^2/A_{44})^2}\,\frac{1}{\rho_Q^2(T_{p2})}\,. \tag{7b}$$

Eq. (7*a*) is only valid to first order in $(T_{p2} - T)$. ΔC_{22} is a renormalization of the fourth order term in ρ_F. Eq. (4*c*) which is exact, shows us that the stabilization of the parameter u at zero in the temperature range $T_{p2} \leqslant T \leqslant T_{p1}$ is due to the CDW-libron interaction (the A_{14} term in eq. (1)) and that the deviation of the parameter u from zero is caused by the inter-subsystem interaction (the A_{12} term in eq. (1)). The neglected bilinear libron-libron parameter (a $A_{34}\,u\chi_Q\,\chi_F$ term in the energy) has the same role as the CDW-CDW parameter A_{12}, thus it can be absorbed in this parameter, as long as it is not too strong.

The transition temperatures, for the region where $T_{p1} > T_{p2}$ [15] are equal to :

$$T_{p1} = T_1 + \Delta T_1\,,\qquad \Delta T_1 = T_1\,A_{14}^2/(\alpha_{11}\,A_{44}) \tag{8a}$$

$$T_{p2} = T_2 + \Delta T_2 + \Delta T_2'\,,\quad \Delta T_2 = T_2\,A_{23}^2/(\alpha_{22}\,A_{33}) \tag{8b}$$

$$\Delta T_2' = T_2(A_{12}^2/\alpha_{22})\,(A_{44}/A_{14}^2)$$
$$\Delta T_2' = T_1\,T_2\,W/\Delta T_1\,,\quad W = A_{12}^2/\alpha_{11}\,\alpha_{22}\,. \tag{8c}$$

Eq. (8*a*) gives us the renormalization of the first transition temperature due to the CDW-libron interaction. This renormalization is always positive. Eq. (8*b*) contains, in addition to the CDW-libron renormalization ΔT_2, a second renormalization $\Delta T_2' > 0$ due to the inter-subsystem coupling. From eq. (8)

$$\Delta T_2' \propto (\Delta T_1)^{-1}$$

and depends therefore upon the electron-libron renormalization in the first sybsystem. Generalization of eq. (8) to the case of the $A_{14}(A_{23})$ parameter depending upon T is discussed in section 3 (eq. 27)).

A feature of the phase diagram follows from the fact that u must be less or equal to one. If for some set of parameters of the LFEF a $u > 1$ solution is obtained from eq. (3), those equations must be replaced by

$$\left.\frac{\partial F}{\partial \eta_i}\right|_{u=1} = 0 \quad i = 1, 2, 3, 4 \quad \left.\frac{\partial F}{\partial u}\right|_{u=1} < 0\,. \tag{9}$$

These equations may define a new phase for which $u = 1$, $\chi_Q = \chi_F = 0$ and the PLD amplitudes (ρ_Q and ρ_F) are non-zero. The zero of the libron order parameters follows from eq. (1) in which the electron-libron coupling disappears for $u = 1$. We discuss this case in section 4.

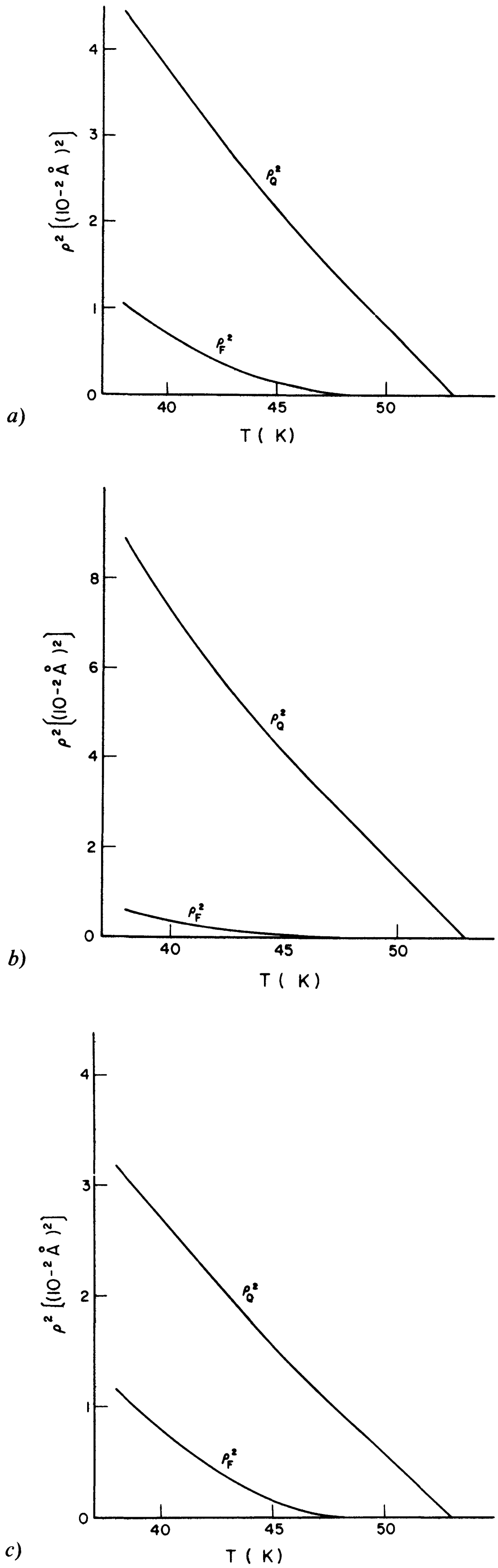

Fig. 2. — The longitudinal displacement amplitudes of the PLD in each type of chains *versus* temperature obtained by solving the minimum conditions for the LFEF with the corresponding sets of interaction parameters listed in table VI.

The numerical solution of the LFEF for the CDW-libron interaction only (eq. (1) with $A_{11}[a] = A_{22}[a] = 0$) is presented here for three sets of parameters A_{12}, A_{14}, and A_{23}. These three sets (see Table VI) fit the temperature dependence of the transverse period but they give different results for the order parameter amplitudes and for values of the specific heat jump at $T_{p1} = 53$ K. A more detailed comparison between these sets of parameters is made in section 5.

Figure 2 represents the temperature dependence of the longitudinal order parameters. ρ_Q^2 behaves according to *classical* Landau theory. The experimental value, derived from the intensity of neutron diffraction lines, shows some saturation, probably due to higher order terms. We feel that the agreement between the present crude theory and experiment is about as good as could be expected. We note that ρ_F^2 has a pronounced non-linear component near T_{p2} due to the closeness of T_{p1}. Figure 3 illustrates the temperature dependence of the libron order parameters. We note that the value of χ_F at 38 K means a linear deviation of the sulphur atom in the TTF-molecule $\delta R_S \approx 1 \times 10^{-2}$ Å which is comparable with the longitudinal displacement ρ_F. The magnitude of the rotation at 0 K is smaller by a factor of 10 from the values measured by Johnson and Watson [37] in TTF_7I_5.

Figure 4 shows the good fit of the transverse period $q_a = 2\pi/\lambda$ as function of temperature to the experimental points.

The heat capacity was also calculated and figure 5 shows its temperature dependence. Between 53 K and 48 K we have the usual mean field behaviour, but under 48 K C_p increases with decreasing temperature and a broad maximum (Fig. 5*c*) appears. This unusual behaviour can be readily understood if eqs. (4*a*), (4*b*) and (4*c*) are used to rewrite the free energy of eq. (1*a*) in the following form :

$$F = F_1(\rho_Q) + F_2(\rho_F) - \frac{A_{12}^2\,\rho_Q^2\,\rho_F^2}{\dfrac{A_{14}^2}{A_{44}}\rho_Q^2 + \dfrac{A_{23}^2}{A_{33}}\rho_F^2}, \quad u < 1 \tag{10a}$$

where

$$F_1(\rho_Q) = \alpha_{11}\frac{(T - T_1 - \Delta T_1)}{T_1}\rho_Q^2 + C_{11}\,\rho_Q^4 \tag{10b}$$

$$F_2(\rho_F) = \alpha_{22}\frac{(T - T_2 - \Delta T_2)}{T_2}\rho_F^2 + C_{22}\,\rho_F^4 \tag{10c}$$

are the *classical free energies* of the ($\rho_Q\,\chi_F$) and ($\rho_F\,\chi_Q$) subsystems respectively. The third term in eq. (10*a*) represents an effective interaction between those two subsystems. In the 48 K-53 K temperature range $\rho_F = 0$, $F = F_1(\rho_Q)$ and the classical solution is obtained for the free energy. Below 48 K the series

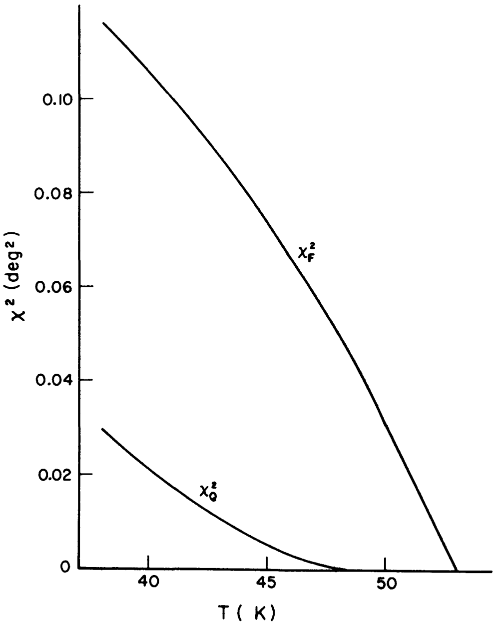

a)

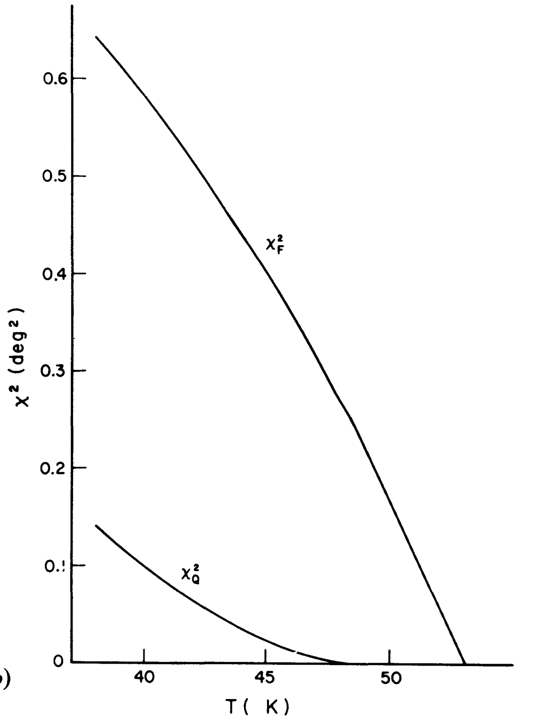

b)

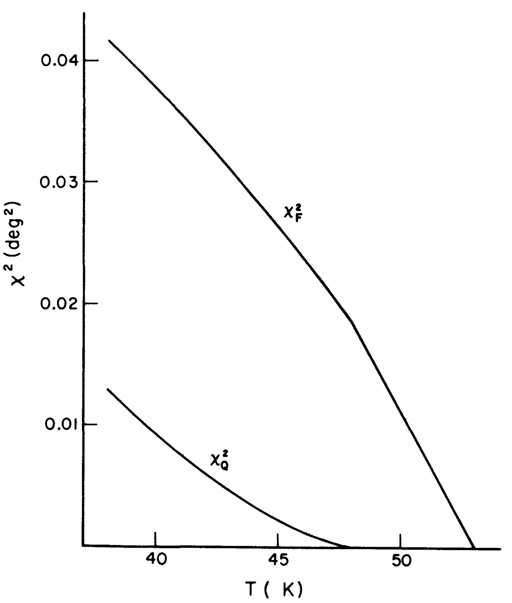

c)

Fig. 3. — The rotational (libronic) order parameters *versus* temperature for the corresponding three sets of interaction parameters.

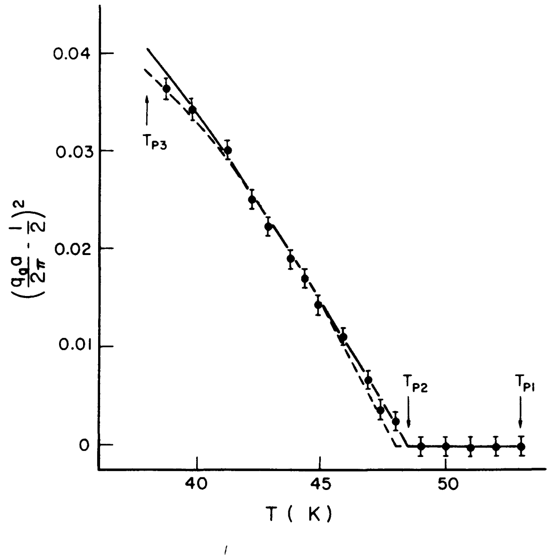

Fig. 4. — Transverse period *versus* temperature. The experimental points are from Ellenson *et al.* [58]. The continuous curve corresponds to the parameters of the set *a* of table VI and the broken line to those of the set *c*.

expansion of the free energy in powers of $(T_{p2} - T)$ may be obtained for the case

$$(T_{p2} - T) \ll (T_{p1} - T_{p2})$$

$$F = F_0(T) - \frac{a}{2}(T - T_{p2})^2 + \frac{b}{3!}(T - T_{p2})^3 + \cdots$$
$$a, b > 0\,, \quad T < T_{p2} \quad (11)$$

where $F_0(T)$ is the free energy for $T \geqslant T_{p2}$. The coefficient of the quadratic term may be obtained with the help of eqs. (7) and (10*b*) and (10*c*). This coefficient is equal to

$$a = \frac{\alpha_{22}^2}{2(C_{22} + \Delta C_{22})\, T_2^2} \quad (12)$$

and is small when T_{p1} and T_{p2} are close (see eq. (7*b*)) and the third order term becomes important. The specific heat below the second phase transition is

$$C_p(T) = C_{p0}(T) + aT - bT(T - T_{p2}) + \cdots \quad (13)$$

where $C_{p0}(T)$ is the specific heat above the phase transition.

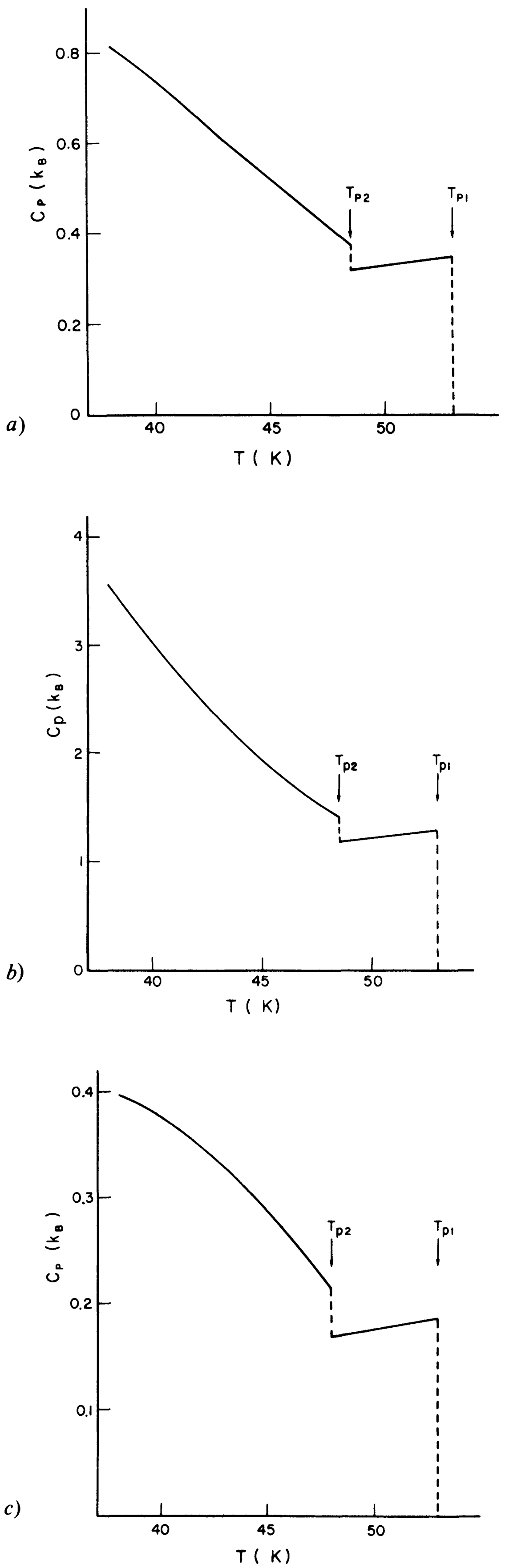

Fig. 5. — The heat capacity C_p *versus* temperature calculated from the minimum conditions for the LFEF with the corresponding sets of parameters listed in table VI.

From eq. (13) we conclude that the heat capacity jump $\Delta C_p(T_{p2})$ at the second phase transition is equal to

$$\Delta C_p(T_{p2}) = aT_{p2} \propto (T_{p1} - T_{p2}) \qquad (14)$$

and it is *small* when T_{p2} is close to T_{p1}.

Below the second phase transition when the a-term in eq. (13) is sufficiently small the derivative of C_p at T_{p2}^- is negative and a broad maximum appears due to the third term in eq. (13). We note that two above-mentioned facts are not specific for our particular model but are the peculiar features of the MF model for two nearby second order transitions.

In the recent measurements of the heat capacity [38] an additional maximum was found at $T \approx 46$ K. The origin of the maximum may well be identified with the closeness of the two successive phase transitions in TTF-TCNQ (see Fig. 5). However, we were not able to obtain a maximum at 46 K by changing three interaction parameters only (see discussion in the end of section 5).

Recently, Craven *et al.* [3] noted that MF theory does not account quantitatively for the jump of the specific heat at $T = 53$ K. They measured

$$\Delta C_p = 0.3\, k_F$$

while the MF theory predicted

$$\Delta C_p \simeq 10 \frac{N(\varepsilon_F)}{N} (k_B\, T_1)\, k_B \approx 0.08\, k_B \text{ for } T_1 = 53 \text{ K}\,.$$

The enhancement of ΔC_p can be readily understood if we note that the quartic coefficient $C_{11} \propto T^{-2}$, and that $T_{p1} = T_1 + \Delta T_1$ rather than T_1 must be used in its evaluation. When the corresponding changes are made in the ΔC_p formula, we get

$$\Delta C_p = 10 \frac{N(\varepsilon_F)}{N} (k_B\, T_{p1}) \left(\frac{T_{p1}}{T_1}\right)^2 k_B \qquad (15)$$

and a bare transition temperature $T_1 \simeq 27$ K can account for the ΔC_p enhancement.

3. Estimation of the parameters of the free energy function.

— In this section we present the calculations of the parameters of the LFEF of eq. (1). As was already mentioned, the microscopic theory of the Peierls transition for the specific case of TTF-TCNQ must include the interaction between conduction electrons and at least four phonon modes.

We aim to express all the parameters in eq. (1) *via* a set of the microscopic quantities such as longitudinal phonon and libron frequencies ω_i ($i = 1, 2$ for the longitudinal phonons and $i = 3, 4$ for the librons), the electronic density of states $N(\varepsilon_F)$, appropriate matrix elements of the interaction, etc. Up to now, however, such a theory has not yet been developed and we approach the problem using the mean field approximation [33, 34, 39, 40, 41, 42] to estimate the parameters α_{ii}, C_{ii} ($i = 1, 2$) and we generalize these theories to estimate the CDW-libron coupling A_{14} and A_{23} and the CDW-CDW A_{12} coupling. The elastic libron parameters A_{33} and A_{44} are estimated using the experimental data on the X-ray Debye-Waller factor [23], the unrenormalized transition temperatures T_1 and T_2, eq. (2), are obtained from eqs. (8*a*), (8*b*) using the experimental values $T_{p1} = 53$ K and $T_{p2} = 48$ K.

To describe the high-temperature phase transition in TTF-TCNQ (an ordering of the (ρ_Q, χ_F) subsystem) we add to the Frohlich Hamiltonian the electron-libron interaction with the TTF η-libron mode [21].

The Hamiltonian which leads to the Peierls transition of the (ρ_Q χ_F) subsystem has the form

$$H = H_e + H_{ph} + H^{long.ph.}_{e-ph} + H^{lib.}_{e-ph} \qquad (16)$$

where the first two terms are the kinetic energy of the electrons and the energy of the phonons. The essential part of the last two terms may be written as follows

$$H^{long.ph.}_{e-ph} + H^{lib}_{e-ph} = \int dx\, dy \psi^+(x, y)\, \psi(x, y) \times \\ \times \left[g_{11}(\mathbf{q})\,(b_{\mathbf{q}} + b^+_{-\mathbf{q}}) + g_{14}(\mathbf{q})\,(a_{\mathbf{q}} + a^+_{-\mathbf{q}}) \right] e^{i\mathbf{q}.\mathbf{r}} \qquad (17)$$

where the q-components are $2\, k_F$ along the chains and q_a along the x-direction (alternating chains). g_{11} and g_{14} stand for the electron-longitudinal phonon and the electron-libron coupling constants, respectively. $\psi(x, y)$ is the electron wave fields, the operators $b_{\mathbf{q}}$ and $a_{\mathbf{q}}$ destroy a longitudinal phonon and a libron, respectively.

We define now the order parameter as half the gap in the electronic spectrum of the TCNQ chains

$$\Delta_1 = \left[g_{11}(\mathbf{q}) \langle b_{\mathbf{q}} + b^+_{-\mathbf{q}} \rangle + g_{14}(\mathbf{q}) \langle a_{\mathbf{q}} + a^+_{-\mathbf{q}} \rangle \right] \times \\ \times e^{i\mathbf{q}.\mathbf{r}} \equiv \Delta_{11} + \Delta_{14} \,. \qquad (18)$$

This order parameter replaces the ABB [39] order parameter (our Δ_{11}). Further, we may follow the previous work [39, 40] and obtain for the free energy the expression

$$F \approx \frac{N_1(\varepsilon_F) \mid \Delta_{11} \mid^2}{\lambda_{11}} + \frac{N_1(\varepsilon_F) \mid \Delta_{14} \mid^2}{\lambda_{14}} + \\ + a_e[\mid \Delta_{11} \mid^2 + 2 \operatorname{Re}(\Delta_{11} \Delta_{14}) + \mid \Delta_{14} \mid^2] \\ + b_e \mid \Delta_{11} \mid^4 + \cdots \qquad (19)$$

where the first two terms are the elastic energies and the other terms appear from the expansion of the electronic part of the free energy in powers of the order parameter. The dimensionless interaction parameters are

$$\lambda_{1i} = 2\, N_1(\varepsilon_F)\, g^2_{1i}(q)/\hbar\omega_i(\mathbf{q}) \quad i = 1, 4 \qquad (20)$$

and $\omega_{1(4)}$ is the phonon (libron) frequency, $N_1(\varepsilon_F)$ is the density of states for one spin direction.

We assume that the conduction electron coupling to the longitudinal phonons is much larger than to librons so the longitudinal phonons go soft first and drive the Peierls transition. In the absence of librons the Peierls temperature T_1 would be the solution of the equation

$$\frac{1}{\lambda_{11}} = -\frac{1}{N_1(\varepsilon_F)}\, a_e(T_1)\,, \quad T_1 = K_1\, \varepsilon_F \exp(-\, 1/\lambda_{11}) \qquad (21)$$

where $K_1 = 2 \div 4$ depending upon the electron band model [39, 40, 41, 42] ($K_1 = 2.28$ for the one-half filled band and $K_1 = 4$ for the free-electron model), and the interference term in eq. (19) renormalizes this temperature (see eq. (8*a*)). To compare eq. (19) with eq. (1) we note that the displacements ρ_Q and χ_F are connected to the order parameters by the equations

$$\rho_Q = \frac{\mid \Delta_{11} \mid}{g_{11}(\mathbf{q})} \left(\frac{\hbar}{2\, M_1\, N\omega_1(\mathbf{q})} \right)^{1/2} \\ = \frac{\mid \Delta_{11} \mid}{\omega_1(\mathbf{q})} \left(\frac{N_1(\varepsilon_F)}{N} \frac{1}{\lambda_{11}\, M_1} \right)^{1/2} \\ \chi_F = \frac{\mid \Delta_{14} \mid}{g_{14}(\mathbf{q})} \left(\frac{\hbar}{2\, I_4\, N\omega_4(\mathbf{q})} \right)^{1/2} \\ = \frac{\mid \Delta_{14} \mid}{\omega_4(\mathbf{q})} \left(\frac{N_1(\varepsilon_F)}{N} \frac{1}{\lambda_{14}\, I_4} \right)^{1/2} \qquad (22)$$

where M_1 is the TCNQ molecular mass and I_4 is the moment of inertia of the TTF molecule around the η-axis and N is the number of cells along the y-axis. Noting that

$$\frac{N_1(\varepsilon_F)}{\lambda_{11}} + a_e(T) = -\, N_1(\varepsilon_F) \ln \frac{T_1}{T} \text{ [39, 40]}\,,$$

we obtain for the coefficients of the LFEF, eq. (1) :

$$\alpha_{11} = NM_1\, \omega_1^2(\mathbf{q})\, \lambda_{11} \qquad (23)$$

$$C_{11} = \frac{N}{2} \cdot K_2 \cdot \frac{(M_1\, \omega_1^2\, (\mathbf{q})\, \lambda_{11})^2}{\dfrac{N_1(\varepsilon_F)}{N} (k_B\, T_{p1})^2} \qquad (24)$$

where the coefficient K_2 depends upon the electron band model. Eq. (24) follows from the explicit expression for b_e, eq. (17) in ref. [39] where $K_2 = 0.106$.

The $\rho_Q\, \chi_F$ term in eq. (1) appears in eq. (19) in the form $2\, a_e(T) \operatorname{Re}(\Delta_{11}\, \Delta^*_{14})$. In the first approximation we put $a_e(T) \approx a_e(T_1) = -\dfrac{N_1(\varepsilon_F)}{\lambda_{11}}$ (see eq. (19)). Using eq. (22) we obtain by comparison with eq. (1) :

$$\mid A_{14} \mid = N\omega_1(\mathbf{q})\, \omega_4(\mathbf{q}) \left(\frac{\lambda'_{14}}{\lambda_{11}}\, M_1\, I_4 \right)^{1/2} \qquad (25)$$

where $\lambda_{14} = \lambda'_{14}(1 - u^2)$.

The parameter A_{14} determines the renormalization of the transition temperature, eq. (8*a*). If the renormalization ΔT_1 is large, the temperature dependence of A_{14} in the interval $T_1 < T < T_{p1}$ cannot be neglected. In this case we obtain instead of the eq. (25) the following expression

$$A_{14}(T) = N a_e(T)\, \omega_1(\mathbf{q})\, \omega_4(\mathbf{q}) \times \times (\lambda_{11}\, \lambda_{14}\, M_1\, I_4)^{1/2} / N_1(\varepsilon_F) \quad (25a)$$

where $a_e(T)$ is a known function (essentially for $T \ll \varepsilon_F$, $a_e(T) \sim \ln \varepsilon_F / T$ [39, 40, 42]). For the phase transition temperature T_{p1} we now have a transcendental equation

$$T_{p1} = T_1 + \frac{A_{14}^2(T_{p1})}{\alpha_{11}\, A_{44}} \quad (26)$$

where $A_{14}(T_{p1})$ is defined in eq. (25*a*). For a given renormalization of the phase transition temperature ΔT_1 we may make a crude estimate of the

$$A_{14}(T_{p1}) / A_{14}^0$$

ratio where A_{14}^0 now is for the value of A_{14} from eq. (25). With the approximation

$$a_e(T) \approx -\frac{N_1(\varepsilon_F)}{\lambda_{11}} + N_1(\varepsilon_F) \frac{T - T_1}{T_1}$$

we obtain the crude estimate

$$A_{14}(T_{p1}) / A_{14}^0 \approx 1 - \lambda_{11} \frac{\Delta T_1}{T_1} \quad (27)$$

and conclude that $| A_{14}(T_{p1}) | < | A_{14}^0 |$. We use eq. (27) in our discussion on the parameters of the LFEF in section 5.

For numerical estimates we use for g_{14} the explicit expression

$$g_{14}(\mathbf{q}) = \left(\frac{\hbar}{2\, I_4\, N \omega_4(\mathbf{q})} \right)^{1/2} M_{14}(\mathbf{q}) \quad (28)$$

where $M_{14}(\mathbf{q})$ is the matrix element of the potential on one electron produced by the libration of a TTF molecule

$$M_{14}(\mathbf{q}) = \int \mathrm{d}^3 r \psi_{\mathbf{k}+\mathbf{q}}^*(\mathbf{r})\, e \left. \frac{\partial V(\mathbf{r}, \chi_F)}{\partial \chi_F} \right|_{\chi_F = 0} \psi_{\mathbf{k}}(\mathbf{r}) \,. \quad (29)$$

The calculation of the matrix element M_{14} was performed for the two above mentioned models of the charge distribution. In the first one we assumed the TCNQ molecular wavefunction of the conduction electron to be localized on the nitrogens, while the net charge of $\mathrm{TTF}^{+0.6}$ molecule was concentrated at the sulphurs [21]. When the nearest neighbour interaction is taken into account the matrix element is given by

$$M_{14}(\mathbf{q}) = 4 \sqrt{1 - u^2} \sin \left(\frac{2\pi}{A} b \right) e \mid c_N \mid^2 \frac{\partial V}{\partial \chi_F} \quad (30a)$$

where $$\left| \frac{\partial V}{\partial \chi_F} \right| = z_S\, e \frac{\partial R_{NS}^{-1}}{\partial \chi_F}$$

is the electrostatic potential at the nitrogen atom due to the net charge of the sulphur atom, c_N is the LCAO coefficient of each of the nitrogens atoms in the molecular wavefunction ($| c_N |^2 = 0.25$), z_S is the net charge at the sulphur atoms ($z_S = 0.6 \times 0.25$), R_{NS} is the distance between nitrogen and sulphur atoms, $\sin \left(\frac{2\pi}{A} b \right) \approx 1$ and the factor 4 appears when summing over the four bridges with the four nearest TCNQ molecules (see Fig. 12). This NS contribution leads to a rather small value of the A_{14} interaction parameter because the centre of the TTF molecule, the N and the S atoms are almost colinear and the motion of the sulphur is almost perpendicular to the NS distance. Therefore, also the end carbon atoms must be included and the A_{14} parameter is determined by the electrostatic potential

$$\frac{\partial V}{\partial \chi_F} = e \left(z_S \frac{\partial R_{NS}^{-1}}{\partial \chi_F} + z_C \frac{\partial R_{NC}^{-1}}{\partial \chi_F} \right).$$

The value of A_{14} (NS only) appearing in table IV was calculated supposing that the net charge in TTF is equally distributed between sulphurs and end carbons ($z_S = z_C = 0.6 \times 0.125$).

We also calculated the $M_{14}(\mathbf{q})$ matrix element taking into account the interaction between the sulphurs and end carbons of the TTF molecule with all the nitrogens in the four nearest TCNQ chains. The summation along these chains diminishes the A_{14} parameter in comparison with the nearest neighbour calculation scheme by 20-30 % (See Appendix I and table IV).

In the second model we allow the charge to be spread over the entire molecule. Eq. (30*a*) is readily generalized and it becomes

$$M_{14}(\mathbf{q}) = 4 \sqrt{1 - u^2} \sin \left(\frac{2\pi}{A} b \right) \sum_i e \mid c_i \mid^2 \frac{\partial V_i}{\partial \chi_F} \quad (30b)$$

where c_i are the normalized expansion coefficients of each atomic function in the LCAO molecular wavefunction $\left(\sum_i | c_i |^2 = 1 \right)$, and

$$\frac{\partial V_i}{\partial \chi_F} = \sum_j e z_j \frac{\partial R_{ij}^{-1}}{\partial \chi_F}$$

is the electrostatic potential at the i-th atom of the TCNQ molecule due to net charges

$$z_j \left(\sum_j z_j = \text{charge transfer} \right)$$

of the atoms of the TTF molecule. We note the difference between the orbital charge density, which is the

Table I. — *Physical constants appearing in different equations of this paper.*

Magnitude	Symbol	Numerical value TCNQ	TTF	Units
Longitudinal phonon frequency [55]	$\omega_i(2\,k_F)$	60	60	cm^{-1}
Molecular mass [56]	M_i	204	204	a.u.
Force constant	$1/2\,M_i\,\omega_i^2(2\,k_F)$	0.14	0.14	$\frac{meV}{(10^{-2}\,Å)^2}$
Electron-phonon interaction parameter	λ	0.2	0.2	—
Electron bandwidth [57]	$4\,t$	0.45	0.3	eV
Charge transfer [12] (electrons per molecule)	ν	0.59	0.59	—
Density of states per spin per molecule	$N(\varepsilon_F)/N$	1.8	2.7	eV^{-1}
Fermi energy	ε_F	0.09	0.06	eV
Scale factor ($\Gamma = \kappa/\rho$)	Γ_i	0.17	0.21	$(10^{-2}\,Å)^{-1}$
Moment of inertia (*), η axis	I_i^η	2140	1175	a.u. $Å^2$
Moment of inertia (*), ζ axis	I_i^ζ	300	—	a.u. $Å^2$
Libron frequency (**), η axis	ω_i^η	52	47	cm^{-1}
Libron frequency (**), ζ axis	ω_i^ζ	51	—	cm^{-1}
Direction cosinuses of the TCNQ	β	0.57	—	—
Rotation χ_Q	γ	0.824	—	—

(*) Calculated with data from ref. [56].
(**) Calculated with data at 100 K from ref. [22].

charge density of the additional π_z electron (or hole) on a given atom (represented by $|c_i|^2$), and the total charge density on a given atom, which also includes the polarization of the cores, and σ-bonds. For example, in neutral TCNQ, the sum of the orbital charges on all atoms vanishes, however, the CN groups have dipole moments (with the nitrogen negative). In $TCNQ^-$, the orbital charge density on the nitrogens is only $-0.061\,e$ while the total charge density is $-0.251\,e$. If we approximate the net charge of the nitrogen in $TCNQ^{-0.6}$ by the linear interpolation between the $TCNQ^0$ and $TCNQ^-$ charges, then $z_N = -0.21$ is obtained. The values of the orbital charge densities $|c_i|^2$ and the atomic total charges densities both for the TTF and TCNQ molecules were calculated with data from ref. [25] and are listed in table II. The M_{14} matrix element was also calculated including the interaction between a TTF molecule and all four nearest TCNQ chains. These results are summarized in table III and IV, and detailed calculations are presented in Appendix I.

The dimensionless electron-libron interaction parameter

$$\lambda'_{14} = \frac{[M_{14}(\mathbf{q})]^2\,N_1(\varepsilon_F)/N}{I_4\,\omega_4^2(1-u^2)} = \frac{[M_{14}(\mathbf{q})]^2\,N_1(\varepsilon_F)/N}{2\,A_{44}(1-u^2)}$$

is found to be equal to 0.02 and 0.13 for the first and the second models, respectively. From eq. (19) $\lambda_{11} \approx 0.2$ so $\lambda_{14}/\lambda_{11} \approx 0.1$-$0.65$. Note that A_{14} depends on the Fermi Energy ε_F and on the transition temperature T_1 only through $A_{14} \propto \left(\ln \frac{K_1\,\varepsilon_F}{T_1}\right)^{1/2}$ (see eq. (19) and eq. (23)), and therefore this quantity is not sensitive to the precise values of ε_F and T_1.

Table II. — *The* LCAO *coefficients c_i of the π-electron of the* TTF *and* TCNQ *molecules and the net charge density z_i of the* $TTF^{0.6}$ *and* $TCNQ^{-0.6}$ *ions. $|c_i|^2$ are the differences between the charge densities of the neutral and the once ionized molecules* (Fig. 13) *and z_i the linear interpolation between them as explained in the text.*

TCNQ	H	C_1	C_2	C_3	C_4	N
$\|c_i\|^2$	0.025	0.037	0.015	0.159	0	0.101
z_i	0.012	− 0.033	0.054	− 0.078	0.093	− 0.211

TTF	C_1	S	C_2	H
$\|c_j\|^2$	0.002	0.178	0.023	0.046
z_j	0.050	0.037	0.021	0.067

In the same way we estimate α_{22}, C_{22}, and A_{23} from eq. (1). The estimate of A_{12} may also be obtained by including a longitudinal phonon in the second chain. This phonon produces change of potential on the conduction electron of the first chain by modulating the R_{NS} and R_{NC} distances. The result of this calculation is analogous to eq. (21) for A_{14} [43]. We obtain

$$|A_{12}| = N\omega_1(\mathbf{q})\,\omega_2(\mathbf{q}) \times \times \left[\left(\frac{\lambda'_{12}}{\lambda_{11}}M_1\,M_2\right)^{1/2} + \left(\frac{\lambda'_{21}}{\lambda_{22}}M_1\,M_2\right)^{1/2}\right] \quad (31)$$

Table III. — *Matrix elements in the nearest neighbours approximation for some chosen pairs of atoms*

$$M_{14}^{*}(ij) = 4 \sin (q_b b) e^2 \mid c_i \mid^2 z_j \frac{\partial R_{ij}^{-1}}{\partial \chi_F}$$

$$M_{23}^{\eta(\zeta)*}(ij) = 4 \sin (q_b b) e^2 \mid c_j \mid^2 z_i \frac{\partial R_{ij}^{-1}}{\partial \chi_Q^{\eta(\zeta)}}$$

$$M_{12}^{*}(ij) = 4 \sin (q_b b) e^2 \mid c_i \mid^2 z_j \frac{\partial R_{ij}^{-1}}{\partial \rho_F}$$

$$M_{21}^{*}(ij) = 4 \sin (q_b b) e^2 \mid c_j \mid^2 z_i \frac{\partial R_{ij}^{-1}}{\partial \rho_Q}$$

Pair (*)	M_{14}^{*} (**)	$M_{23}^{\eta *}$ (**)	$M_{23}^{\zeta *}$ (**)	M_{12}^{*} (***)	M_{21}^{*} (***)
—	—	—	—	—	—
NH	2.98	4.87	0.05	– 0.018	0.025
NC_2	0.53	1.82	– 0.13	0.004	– 0.010
NS	0.08	13.34	– 3.80	0.044	– 0.440
C_4H	0.00	– 0.94	– 0.01	0.000	0.010
C_4C_2	0.00	– 0.39	0.02	0.000	0.008
C_4S	0.00	– 3.47	0.56	0.000	0.171
C_3H	1.46	0.36	0.00	0.028	– 0.009
C_3C_2	0.32	0.15	0.00	0.010	– 0.005
C_3S	0.24	1.42	0.00	0.040	– 0.095

(*) The first (second) atom in each pair belongs to the TCNQ(TTF) molecule and the nearest of all the pairs bearing the same symbol is meant.

(**) The values of the CDW-libron matrix elements are given in meV/deg. and the charge densities are those of table II.

(***) The values of the CDW-longitudinal phonon matrix elements are given in meV/(10^{-2} Å).

Table IV. — *Theoretical estimations of the* CDW-*libron* LFEF *parameters.*

a) *One chain parameters*

	$\alpha \left(\frac{\text{meV}}{(10^{-2}\,\text{Å})^2}\right)$	$C \left(\frac{\text{meV}}{(10^{-2}\,\text{Å})^4}\right)$	$A_{ii} \left(\frac{\text{meV}}{\text{deg.}^2}\right)$ (*)
	—	—	—
TCNQ	0.055	0.004 2	1.4
TTF	0.055	0.003 4	1.5

(*) A_{33} and A_{44} for TCNQ and TTF respectively.

b) *Interaction parameters*

	The first (NS) model		The second (all pairs) model	
	NN	Chain	NN	Chain
	—	—	—	—
$A_{14}^{0}\left(\frac{\text{meV}}{10^{-2}\,\text{Å deg.}}\right)$	0.25	0.20	0.75	0.30
$A_{23}^{0}\left(\frac{\text{meV}}{10^{-2}\,\text{Å deg.}}\right)$	0.54	0.42	0.94	0.83
$A_{12}(\text{CDW})\left(\frac{\text{meV}}{(10^{-2}\,\text{Å})^2}\right)$	—	0.036	—	0.84
$A_{12}(\text{interf.})\left(\frac{\text{meV}}{(10^{-2}\,\text{Å})^2}\right)$	0.050	0.033	0.10	0.05

NN and chain stand for *nearest neighbours calculation* and *summing along the chain calculation* respectively.

where $\lambda_{12} = \lambda'_{12} u$, $\lambda_{21} = \lambda'_{21} u$, M_2 is the TTF molecular mass, and the matrix element that determines the λ_{12} coupling constant (see eq. (20), $i = 2$, and eq. (28)), is :

$$M_{12} = \int \psi_{\mathbf{k}+\mathbf{q}}(\mathbf{r}) \frac{\partial V(r, \rho_F)}{\partial \rho_F}\bigg|_{\rho_F = 0} \psi_{\mathbf{k}}(\mathbf{r})\, d^3 r .$$

The explicit expression for $M_{12}(q)$ in the tight binding approximation follows from eq. (30*a*) by replacing $(1 - u^2)^{1/2}$ by u and χ_F by ρ_F. The numerical estimate of A_{12} is presented in table IV ($\lambda'_{12} \sim \lambda'_{21} \sim 10^{-3}$).

All our numerical estimates of the interaction parameters in eq. (1) are based only on monopole-monopole nearest neighbour interactions between TTF and TCNQ molecules. Polarization leads also to monopole-dipole, dipole-dipole interactions [21], etc. It is worthwhile to note that the effective charge z_N (and z_S) is also somewhat modulated by the phonons (librons), (see ref. [21], section 2). The modulation of the effective charge by the phonons also contributes to the Frohlich coupling constant. This effect follows directly from the phonon (libron) modulation of the expansion coefficients of the LCAO wave function of the chain [44]. We do not consider that effect here.

We have also neglected the intramolecular screening of the interaction between the charges localized on atoms which do not lie on the periphery of the molecules. That is why the more simpler first model which uses only the charges on the periphery of the TTF and TCNQ molecules is useful as a kind of limiting case. We return to this question in section 4. The values of some physical quantities needed for the calculations of the different interaction parameters are listed in table I.

We note that all interaction parameters above estimated are of the interference nature. But the A_{12} parameter has another contribution which follows from the direct CDW-CDW Coulomb interaction of two different stacks. Therefore we can write

$$A_{12} = A'_{12} + A''_{12}$$

where the first is the CDW-CDW contribution and the second is from eq. (31). We estimate the first term in the next section (see also Appendix II). Here we note that these two parts differ in their dependence upon the charge transfer

$$A'_{12} \propto \cos\left(\frac{2\pi}{\Lambda} b\right) \quad \text{and} \quad A''_{12} \propto \sin\left(\frac{2\pi}{\Lambda} b\right).$$

So the A_{12} interaction vanishes not exactly for the 1/4 filled band but for $q_b = 2\pi/\Lambda$ which depends upon the ratio A''_{12}/A'_{12}. Our estimate (see next section) shows that the interference mechanism (eq. (31)) contributes about 5 to 10 % to the A_{12} interaction parameter (see Table IV).

In view of all the approximations used for the estimate of the interaction parameters we believe that they are accurate within a factor of about two.

The parameters A_{33} and A_{44} follow from experiment [22] where the mean square amplitude of the TTF and TCNQ librations were measured. The experimental uncertainties are about 30 % and our choice of the A_{44} and A_{33} parameters corresponds to the values of the force constants for a temperature of 100 K. The experimental data [22] for the TCNQ molecule show that the elastic restoring force for the η-libration is much larger (11 eV/rad.^{2}) than for the ζ-librations (1.4 eV/rad.^{2}). This fact leads to the redefinition of the libron coordinate χ_Q. Indeed, geometrically the η-libration is the most important factor in the modulation of the S-N distance [21] but because of the relative small amplitudes of this libration and the large amplitude of the ζ-librations, the last must be included in the electron libron free energy. The straightforward inclusion of the additional order parameter in eq. (1) would complicate the free energy. Therefore, we redefine the χ_Q-librations as rotations around an intermediate axis between the η and ζ ones, and find the direction cosines β and γ by minimizing the part of the free energy that depends only upon χ_Q.

This procedure gives $A_{23} = A^{\eta}_{23}\beta + A^{\zeta}_{23}\gamma$ and $A_{33} = A^{\eta}_{33}\beta^2 + A^{\zeta}_{33}\gamma^2$ with $\gamma/\beta = (A^{\eta}_{33}/A^{\zeta}_{33})/(A^{\eta}_{23}/A^{\zeta}_{23})$. Taking [22] $A^{\eta}_{33} = 11$ eV/rad.^{2}, $A^{\zeta}_{33} = 1.4$ eV/rad.^{2} and estimating $A^{\eta}_{23}/A^{\zeta}_{23} \approx 5.5$ we get $\beta = 0.57$ and $\gamma = 0.824$ which lead to the parameters A_{23} and A_{33} in table IV.

Similarly, ρ_F is a linear combination of a longitudinal phonon and a transverse phonon (polarized in the c^*-direction), as found from experiment in TTF-TCNQ [36], but in the present estimates of the LFEF parameters, we took the ρ_F as a pure longitudinal order parameter.

4. **Direct Coulomb interaction model.** — In this section we calculate the CDW-CDW interaction parameters for the nearest and the next nearest chains, A_{12} and $A_{11}[a]$ ($A_{22}[a]$) respectively. (See also Appendix II.) These parameters were estimated by Bjelis and Barisic [15] but for the continuum model of the CDW (a linear CDW along the b-axes). We develop here a method of calculation of these parameters which takes into account the geometry of the molecules. For the nearest chain parameter A_{12} the geometry factors are essential (we obtain an order of magnitude reduction of the A_{12} parameter compared to the results of ref. [15]). To be closer to the papers which treat the phase transitions in TTF-TCNQ [13, 14, 15] we use here instead of the displacement order parameters ρ_Q and ρ_F the order parameters κ_Q and κ_F related to them. The latter are the CDW amplitude relative to the average charge transfer ν. To be specific we use in the case of the κ order parameters the small letters for labeling the LFEF parameters in eq. (1a) (e.g. a_{12}, $a_{11}[a]$, c_{11} and so on). We first determine the relation between the CDW parameter κ and the displacement parameter ρ used in eq. (1).

If we expand the electron density on a chain, $n(y) = \sum_{k,\sigma} |\psi_{k\sigma}(y)|^2$, in a Fourier series

$$n(y) = n_0\left(1 + \sum_{q>0} \kappa_q \cos(qy + \varphi_q)\right)$$

components κ_q with $q \neq n\frac{2\pi}{b}$ (n integer) appear in the case of a non-commensurate CDW. We define the CDW parameter κ in the case of the usual Peierls transition by the equality $\kappa = |\kappa_{2k_F}|$.

To calculate a *one-chain* parameter a_{ii} and c_{ii}, $i = 1,2$, it is sufficient to calculate the ratio $\Gamma = \kappa/\rho$ for a chain. With given Γ the one-chain parameters may be obtained by the simple scaling of eq. (23) and eq. (24). In the frame of the one-electron MF-theory [33, 34, 39, 40], it is a simple matter to prove that

$$\kappa = \frac{N(\varepsilon_F)}{\nu N}\frac{2|\Delta|}{\lambda} \tag{32}$$

where νN is the number of electrons in a chain and Δ is defined by eq. (18) with $g_{14} = 0$. From eq. (22) and eq. (32) we obtain

$$\Gamma = \frac{2}{\nu}\left(\frac{N.(\varepsilon_F)}{N}\frac{M\omega^2}{\lambda}\right)^{1/2} \tag{33}$$

where ω is the longitudinal phonon frequency. For the values of the constants listed in table I,

$$\Gamma \simeq 0.2\,(10^{-2}\,\text{Å})^{-1}.$$

Eq. (32) has a simple meaning. Because

$$\frac{N(\varepsilon_F)}{N} \propto \varepsilon_F^{-1}$$

we see that $\kappa \propto \frac{1}{\lambda} \frac{2\,|\,\Delta\,|}{\varepsilon_F}$. For free 1d electrons

$$\kappa = \frac{1}{4\,\lambda} \frac{2\,|\,\Delta\,|}{\varepsilon_F} \quad \text{and if} \quad \lambda \simeq 0.2\,, \quad \kappa = k \frac{2\,|\,\Delta\,|}{\varepsilon_F}$$

and from eq. (32) and table I we obtain $k = 1.4$. Table V presents the LFEF parameters a_{ii} and c_{ii} as scaled from the related parameters of table IV of the LFEF of eq. (1).

Table V. — *Parameters of the free energy function for the direct Coulomb interaction model.*

α_{11}	α_{22}	c_{11}	c_{22}
2 meV	1.3 meV	5.6 meV	1.9 meV

	$a_{11}(a)$	$a_{22}(a)$	a_{12}
NS only	4.3 meV	4.9 meV	1 meV
all bridges	2.7 meV	3.8 meV	23 meV

The calculations of the CDW-CDW interaction parameters using the discrete CDW model and taking into account the atomic structure of TTF-TCNQ, are explained in Appendix II. Also in this calculation, we use two models for the charge distribution. The next nearest chains parameters $a_{11}[a]$ and $a_{22}[a]$ are not sensitive to the actual charge distribution over the molecules (and the continuum model is not too bad for them) but the a_{12} parameter increases about 20 times for the second model compared with the first one. This is not an accidental effect. As shown in ref. [21] the a_{12} interaction in the first (NS) model is weak mainly because the sum of the projection of the nitrogen-nitrogen distance in the TCNQ molecule along the b-axis and the sulphur-sulphur distance in the TTF molecule is approximately equal to half the wavelength of the CDW ($\Lambda = 2\,\pi/2\,k_F$).

Because of the effect of the intramolecular screening much of the non-nearest neighbour pair interactions are screened. Thus the true value of the a_{12} CDW-CDW interaction parameter must lie between these estimates. Because of the large difference between them we took this parameter as a fitting parameter (see next section).

Table V presents the results of the calculations of the DCI parameters. The CDW-libron interaction parameters A_{14} and A_{23} are much less sensitive to the charge distribution model than the CDW-CDW A_{12} interaction parameter (see Table IV). This is due to the fact that the relative tilting of the TTF and TCNQ molecules nearly cancels the NS and NC (end carbons) interactions in A_{12} while there is no such a cancellation in A_{14} and A_{23} (a factor

$$\sin\left[q_b(y_N - y_S)\right] \simeq 1$$

appears in the A_{14} and A_{23} calculations and

$$\cos\left[q_b(y_N - y_S)\right] \ll 1$$

in the A_{12} one).

5. The fitting procedure (which mechanism is responsible for the 3d ordering in TTF-TCNQ ?).

— As follows from the previous sections (section 3 and section 4) our estimations of the interaction parameters are not sufficiently precise to expect them to fit the available experimental information exactly. Therefore, we try to find a best set of three interaction parameters (for instance, A_{14}, A_{23} and A_{12} or $a_{11}[a]$, $a_{22}[a]$ and a_{12}) to fit some experimental measurements and then we compare this best set (set a in table IV) with our theoretical estimates. Note that we fix the other parameters of the LFEF, (eq. (1)) at their theoretical estimates (see table IV). Along with the best set we also solve the LFEF, eq. (1a), for two other sets of three interaction parameters and compare the results. We first discuss the CDW-libron mechanism and then the DCI model.

The available experimental evidence is scarce ; the measured phase transition temperatures [6, 11, 58] (T_{p1} and T_{p2}), the temperature dependence of the transverse period $q_a(T)$ [4, 12, 58]. and the specific heat anomaly [3, 38].

The jump of the specific heat $\Delta C_p(T_{p1})$ at the high temperature phase transition determines with the help of eq. (15) the unrenormalized phase transition temperature T_1 and this *via* eq. (8a) determines the interaction parameter A_{14}. Two other parameters, namely, A_{23} and A_{12} were chosen to fit the initial slope and the curvature of the $q_a(T)$ dependence [58], Thus, set a (Table VI) is chosen to fit both the $\Delta C_p(T_{p1})$ jump (see Table VI) and the $q_a(T)$ dependence (see Fig. (4)). At first sight the correspondence between the parameters A_{23} and its theoretical estimate A_{23}^0 is very poor. But if we pay attention to the large renormalization of the transition temperature (see Table VI, $T_{p2} - T_2 = 39$ K) we conclude that the temperature dependence of the A_{23} parameter between T_{p2} and T_2 is not negligible. As was explained in section 3 in this case $A_{23}(T_{p2}) < A_{23}(T_2) = A_{23}^0$. We can estimate A_{23}^0 with the help of eq. (27) for the given value of the A_{23}. For the coupling constant $\lambda = 0.2$ and $\Delta T_2 = 39$ K we obtain

$$A_{23}^0 \approx A_{23}\left(1 - \lambda \frac{\Delta T_2}{T_2}\right) = 0.97 \frac{\text{meV}}{10^{-2}\ \text{Å deg.}}$$

which is close to our theoretical estimation of A_{23}^0. The A_{14} parameter value from the set a is not very different from the theoretical estimate for the case

Table VI. — *Sets of interaction parameters which were used in the numerical calculations. Set a is the best fit, sets b and c are for illustrative purposes. The unrenormalized transition temperatures, order parameter amplitudes and the specific heat jump at* 53 K *are also listed.*

	a	b	c
$A_{14}(T_{p1})\left(\dfrac{\text{meV}}{10^{-2}\ \text{Å deg.}}\right)$	0.3 (*)	0.5	0.21
$A_{23}(T_{p2})\left(\dfrac{\text{meV}}{10^{-2}\ \text{Å deg.}}\right)$	0.29 (*)	0.85	0.18
$A_{12}\left(\dfrac{\text{meV}}{(10^{-2}\ \text{Å})^2}\right)$	0.09	0.46	0.036
$A_{14}^2/A_{44}\left(\dfrac{\text{meV}}{(10^{-2}\ \text{Å})^2}\right)$	0.06	0.17	0.03
T_1 (K)	25	13	35
T_2 (K)	10	1.5	22
ρ_Q (38 K) (10^{-2} Å)	2.1	3	1.8
ρ_F (38 K) (10^{-2} Å)	1	0.8	1
χ_Q (38 K) (deg.)	0.17	0.4	0.1
χ_F (38 K) (deg.)	0.34	0.8	0.2
ΔC_p (53 K) (k_B) (**)	0.34	1.3	0.19

(*) Corresponding to unrenormalized values $A_{14}^0 \simeq 0.38$ and $A_{23}^0 \simeq 0.97$ as explained in the text (see eq. (27)).

(**) To be compared with the experimental value [3]

$$\Delta C_p\ (53\ \text{K})\ \text{exp} \approx 0.3\ k_B\ .$$

of the chain integration (see Table IV). The renormalization of the T_{p1} temperature is not as large as in the previous case ($\Delta T_{p1} \simeq 20$ K) and we obtain for the same $\lambda = 0.2$

$$A_{14}^0 \simeq 0.38\,\frac{\text{meV}}{10^{-2}\ \text{Å deg.}}\,.$$

Thus the libron-CDW parameters from the set a are in good agreement with the theoretical estimate.

As was discussed at the end of the previous section, it is rather difficult to obtain a precise theoretical estimate of the CDW-CDW interaction parameters.

In fact, the first (N-S) model and the second (the unscreened all pairs interactions) model give the lower and upper bound, respectively. The value A_{12} appearing in the set a (Table VI) falls in between these two estimates.

The temperature dependence of the order parameters, the transverse q_a wave vector and the specific heat anomaly ΔC_p are shown in the figures 2*a*, 3*a*, 4 and 5*a* and were discussed in section 2.

As was mentioned in section 2 it was not possible to reproduce the maximum of the heat capacity at 46 K, for the parameters of the set a it appears at a certain temperature below 38 K. The smallness of the jump $\Delta C(T_{p2})$ at the second phase transition is due to the proximity of the two transition temperatures as was already explained in section 5. It is important to investigate if it is possible to obtain both the maximum at 46 K, the experimental values of the jumps ΔC_p and the $q_a(T)$ dependence simultaneously in the frame of the LFEF, eq. (1). Because all the $C_p(T)$ behaviour depends upon the renormalization of the phase transition temperatures it is better to postpone this investigation until the interaction in the c^*-direction will be included. Of course, additional experimental measurements of the $C_p(T)$ are very desirable.

We have also solved the LFEF for illustrative purposes for another two sets of interaction parameters. These two sets and some results are listed in table VI (column b and c), and the corresponding graphs appear in figures 2*b* and *c*, 3*b* and *c*, 4 and 5*b* and *c*. The set b consists of large interaction parameters while the set c consists of small ones. Both fit the temperature dependence of the transverse period. The set b is characterized by large transition temperature renormalizations which enhance the specific heat jump at 53 K and diminish the ρ_F^2/ρ_Q^2 ratio (see eqs. (6*a* and *b*)). Rather large libronic amplitudes are obtained. The set c shows the effects of smaller interaction parameters.

The LFEF was also solved in terms of the DCI model alone (i.e. the CDW-libron interaction parameters A_{14} and A_{23} were taken equal to zero). Our results showed that if a_{12} were chosen to be half of the estimated value summing over all the possible pairs ($a_{12} = 10$ meV) and the direct interaction between similar chains were the same as calculated (see Table V) then the temperature dependence of the transverse period could be fitted. This set of parameters is equivalent to the above mentioned set b in the sense of the correspondence relations of eq. (5*a*) and eq. (5*b*) (i.e. $2\,A_{11}[a] = 0.16\,\dfrac{\text{meV}}{(10^{-2}\ \text{Å})^2}$ plays the same role as $A_{14}^2/A_{44} = 0.17\,\dfrac{\text{meV}}{(10^{-2}\ \text{Å})^2}$ in in the set b and analogously for

$$\left. 2\,A_{22}[a] = 0.34\,\frac{\text{meV}}{(10^{-2}\ \text{Å})^2}\right)\,.$$

The difference between the DCI model solution and the CDW-libron solution (set b) appears in the unrenormalized transition temperature T_1 which is larger in the former because only

$$A_{11}[a] = 0.08\,\frac{\text{meV}}{(10^{-2}\ \text{Å})^2}$$

enters in the renormalization eq. (5*a*). Therefore, the specific heat jump in the DCI model ($\Delta C_p \approx 0.5\ k_B$) is closer to the experimental value than that obtained in set b.

To complete this discussion we show in figures 6*a* and 6*b* the contour lines and the three dimensional view of the CDW-libron LFEF with the best set of

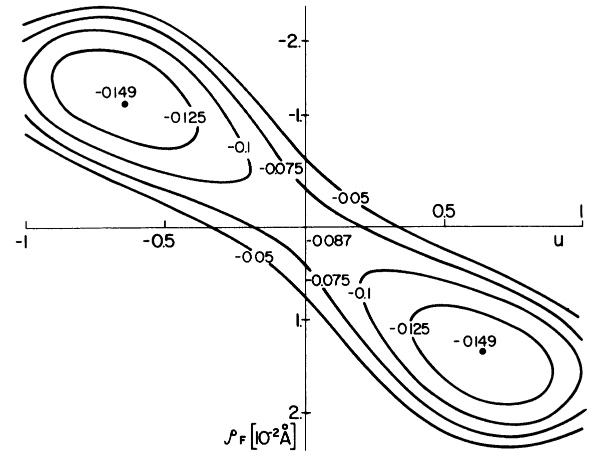

a)

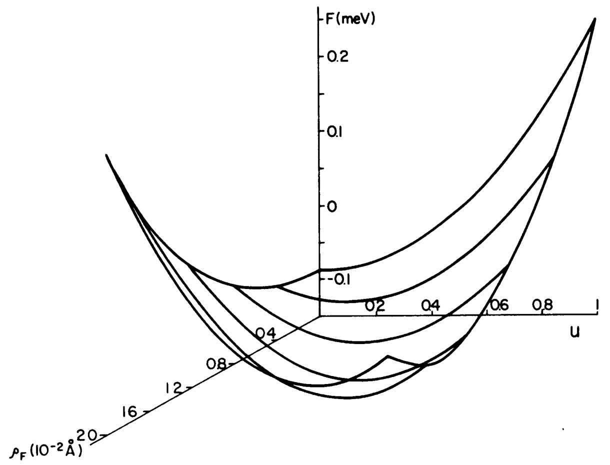

b)

Fig. 6. — The LFEF of eq. (1) with the parameters of the set *a* as function of ρ_F and $u = \cos(q_a\, a/2)$ for $T = 35$ K and

$$\rho_Q = 2.4 \times 10^{-2}\ \text{Å}.$$

a) Contour lines graph. The energy levels are shown in meV. *b*) Three dimensional view.

parameters (Table VI*a*) at a temperature $T = 40$ K. We feel that figure 6*a* and 6*b* deserve some detailed considerations. When we go along the line $\rho_F = 0$ the free energy has a minimum at $u = 0$ ($q_a = 2\pi/2a$), i.e., a $2a$ period. Similarly, when we go along the $u = 0$ line the free energy has a minimum at $\rho_F = 0$. Therefore, it is frequently argued that this is a *theoretical proof* that the point $u = \rho_F = 0$ is a minimum of the free energy and explains the experimental observation of this state in the temperature range 48 K-53 K. Inspection of figures 6*a* and 6*b* shows that this proof is fortuitous. The point $u = 0$, $\rho_F = 0$ is a saddle-point of the free energy and for a diagonal line it is maximum.

From the present numerical estimates it is not possible to decide unambiguously whether the CDW-libron or the DCI mechanism or both are responsible for the 3d ordering. But the screening effects (dielectric constant of the material) diminish the next nearest chain interaction parameters $A_{11}[a]$ and $A_{22}[a]$ significantly.

The nearest chain interaction parameters A_{14}, A_{23} and A_{12} are not influenced by the screening very much. Thus when screening effects upon the $A_{11}[a]$ and $A_{12}[a]$ parameters are significant, only the CDW-libron mechanism can provide the coupling which drives the 3d ordering in TTF-TCNQ.

However, the main difference between the CDW-libron and the DCI model manifests itself in the pressure dependence, since A_{33}, A_{44} increase rapidly under pressure, while $A_{ii}[a]$, $i = 1,2$ should not be strongly pressure dependent. This point will be elaborated in a subsequent publication.

6. The possible phase diagrams for TTF-TCNQ systems. Lifshitz points.

— To obtain a theoretical phase diagram from first principles, the T, P dependence of the parameters of the LFEF must be known in detail. At this stage, we discuss qualitatively some possibilities for the phase diagram in the T-P plane (or in a T-external parameter plane). Somewhat analogous phases (without the libronic order parameter) were already mentioned by Bjelis and Barisic [15]. The complexity of the observed phase diagram [7, 8, 45] is probably a result of the complicated pressure variation of several terms in the LFEF. At this preliminary stage, we discuss an idealized situa-

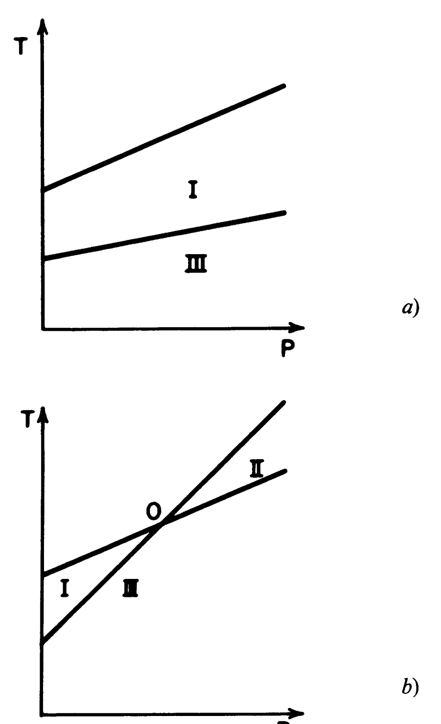

Fig. 7. — Two possible phase diagram of the decoupled ($\rho_Q\, \chi_F$) and ($\rho_F\, \chi_Q$) subsystems. *a*) Divergent transition lines. *b*) Convergent transition lines with quadruple point.

tion, where only one or two terms in the LFEF are varied arbitrarily.

In the case when $A_{12}/(A_{14}^2/A_{44}) < 1$ it is natural to start from the decoupled subsystems $(\rho_Q \chi_F)$ and $(\rho_F \chi_Q)$ (see section 2). If $A_{12} = 0$ we would expect two topological distinct cases. In one case, the $T_{p1}(P)$ and $T_{p2}(P)$ lines are divergent (see Fig. 7*a*). In the second case (Fig. 7*b*) there is a crossing point, $T_{p1} = T_{p2}$, where the disordered and three ordered phases coexist. According to the Gibbs phase rule [46] $r \leqslant 2 + f$ at equilibrium where r is the number of the phases and f is the number of the components. For TTF-TCNQ, $f = 1$, so the quadruple point violates the Gibbs phase rule. In reality, a coupling between the two subsystems (through $A_{12} \neq 0$ in our case) splits the quadrupole point into two triple points. Two topologically different possibilities for this splitting are shown in figures 8*a* and 8*b*. In figure 8*a*, the AB line which divides the disordered phase and the completely ordered phase III is a λ line of second order phase transition points. The A'B' lines in figure 8*b* dividing the $(\rho_Q \chi_F)$ and $(\rho_F \chi_Q)$ phases must be a first order transition line because of the different, symmetry of these two phases.

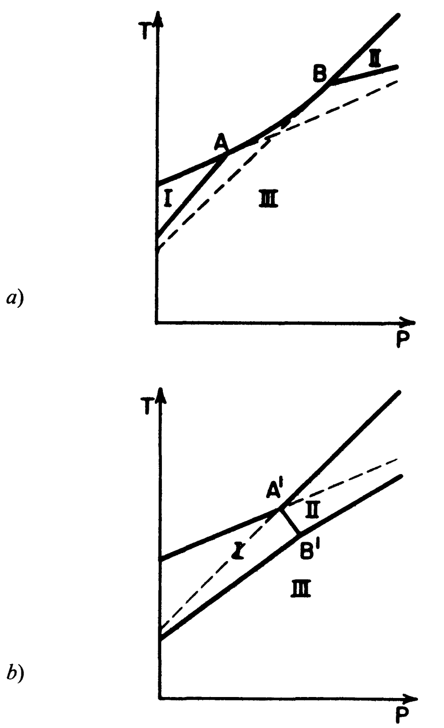

Fig. 8. — Two possibilities for the quadruple point, figure 9*b* being split by a weak inter-subsystem coupling. *a*) Attractive renormalization. *b*) Repulsive renormalization.

In the region of the phase diagram where $T_{p2} > T_{p1}$ (the $(\rho_F \chi_Q)$ phase) we can use eqs. (4)-(8) by changing index 1 for 2. It is obvious that phase I (see Fig. 8*a*) may appear when

$$T_{p1} = T_1 + \Delta T_1 > T_2 + \Delta T_2 + T_1\, T_2\, W/\Delta T_1 = T_{p2} \quad (34)$$

and phase II may appear only if

$$T_{p2} = T_2 + \Delta T_2 > T_1 + \Delta T_1 + T_1\, T_2\, W/\Delta T_2 = T_{p1} \quad (35)$$

where W is given by eq. (8*c*).

It is clear that the inter-subsystem interaction renormalizes the second transition temperature towards the first as is shown in figure 8*a*. So we are now in the position to argue, that for our model (eq. (1)), only the phase diagram of the type shown in figure 8*a* is possible. Indeed, for obtaining the diagram of figure 8*b* from the diagram of figure 7*b* one needs a negative inter-subsystem renormalization (for instance, in the $T_{p1} > T_{p2}$ case one needs $T_{p2} = T_2 + \Delta T_2 - |\Delta T_2'|$). It is possible to obtain such renormalization if a term like $C_{1122}(u)\, \rho_Q^2\, \rho_F^2$ with $C_{1122}(u) > 0$ is included in eq. (1). But at the quadruple point all the order parameters are zero and therefore the renormalization of the transition temperature by the biquadratic term is negligible in the vicinity of the quadruple point. So a splitting of the quadruple point into two multi-critical points A' and B' (as in figure 8*b*) is unlikely.

As was mentioned in section 2 (eq. (9)) a fourth phase is possible for $u = 1$ ($\chi_Q = \chi_F = 0$, $\rho_Q\, \rho_F \neq 0$). The line dividing regions of phase III and this new phase IV may intercept the AB line of figure 8*a* at two new multi-critical points C and D (see Fig. 10). Because phase III is a phase with no commensurate transverse period, the four multi-critical points A, B, C and D can be identified as of Lifshitz type which were introduced by Hornreich *et al.* [24] in connection with magnetic systems. We note that point A (Fig. 8*a*) is consistent with the group theoretical considerations of E. Abrahams and I. Dzyaloshinskii [17].

It is interesting to note that in the vicinity of the Lifschitz point A the quadratic $(T_{p2} - T)^2$ contribution is essential in ρ_F^2. This may be seen from eq. (7*b*) where the renormalization ΔC_{22} of the fourth-order constant in eq. (1) becomes very large near the point $A(\rho_Q^2(T_{p2}) \to 0$ when $T_{p2} \to T_{p1})$.

Concerning the first uncoupled case (Fig. 7*a*), we may expect here several possibilities when the interaction A_{12} is switched on. In the first one, the strong renormalization of the T_2 temperature leads to the monotonic increase of T_{p2} with the external parameter (say, pressure) so that the Lifshitz point is reached (Fig. 9*a*). The other alternative is the fall of the $T_{p2}(P)$ line. In this case, the Lifshitz point also may be reached after the initial divergence of the T_{p1} and T_{p2} lines (see Fig. 9*b*). Theoretically, the renormalization may be so weak that the topological character of the picture, figure 7*a* will not change.

To illustrate the general picture we present in figure 10 the numerical calculations of T_{p1} and T_{p2} as function of the difference $(T_2 - T_1)$ for a highly idealized case when T_i $(i = 1, 2)$ were changed only in the differences $(T - T_i)$ to which the parameters A_{ii}

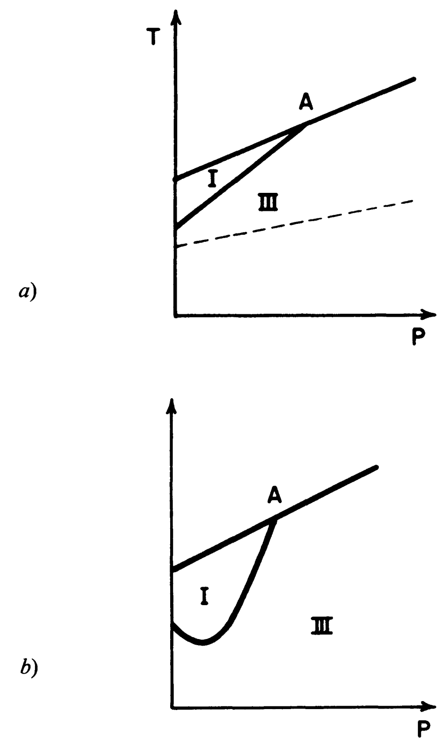

Fig. 9. — Two possible phase diagrams of the coupled ($\rho_Q \chi_F$) and ($\rho_F \chi_Q$) subsystems which follow from the divergent case, figure 9*a*. *a*) Strong attractive renormalization. *b*) Crossover from the pronounced divergent regime to the convergent one.

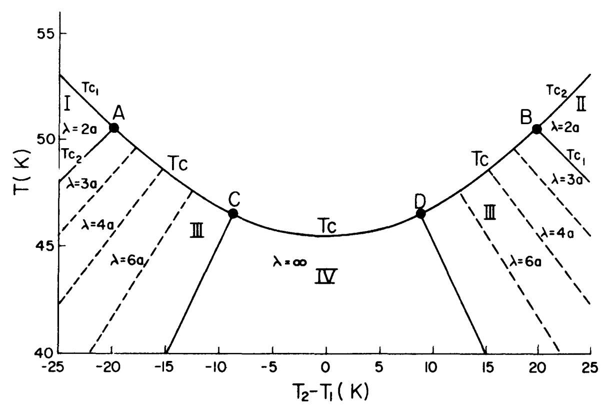

Fig. 10. — The illustrative phase diagram of the TTF-TCNQ-like systems. The full lines are the second order transition lines dividing the following phases : I-($\rho_Q \chi_F$) phase, II-($\rho_F \chi_Q$) phase, III-($\rho_Q \chi_F \rho_F \chi_Q$) phase, IV-($\rho_Q \rho_F$) phase with $u = 1$, $\chi = 0$. The broken lines correspond to constant transverse period ($\lambda = 2 \pi/q_a$).

are proportional, and the other parameters were kept fixed. Figure 11 presents another phase diagram in which only the inter-subsystem interaction parameter is changed and the rest of the parameters are the same as those listed in table I. In this graph two Lifshitz points appear.

Returning to the P-T phase diagram, we note that extensive experimental work on the phase diagram of TTF-TCNQ under pressure has been carried out

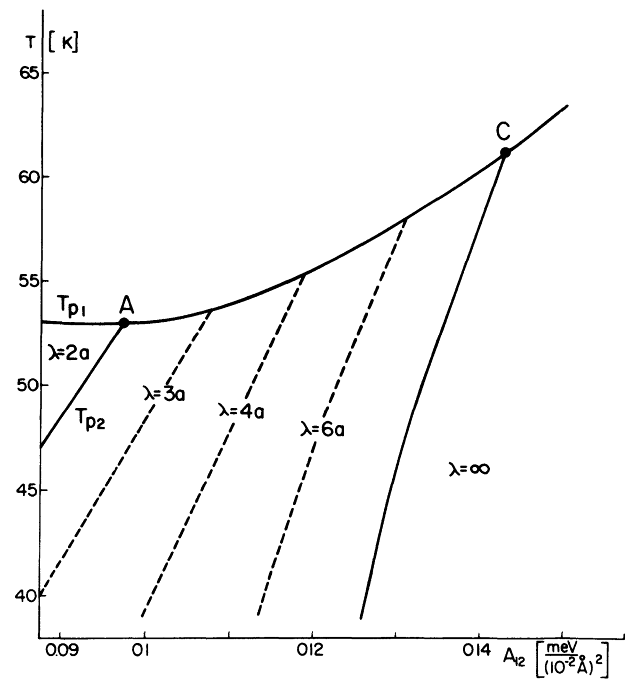

Fig. 11. — The two high temperature transition temperatures of TTF-TCNQ as function of A_{12} showing two Lifshitz points.

in Orsay [7, 8, 45]. The phase diagram is found to be rather complicated. The upper transition temperature T_{p1} (the Peierls transition of the TCNQ stack) increases with pressure from 53 K, at first slowly (0.7 K per kbar), and around 20 kbar there is a sharp maximum of about 70 K, followed by a drop, and than a plateau at about 65 K. The second transition temperature T_{p2} (the Peierls transition of the TTF stack) seems to fall rapidly at low pressures, as manifested by a rather low resistivity, which is only weakly temperature dependent (see figure 2 of Ref. [45], and figure 1 of Ref. [8] for example). At 15 kbar, and above, there seems to be only one transition, so that T_{p2} must have risen sharply with P in this region. There is a first order transition at 38 K [8, 12] which falls rapidly with pressure (about 1 K per kbar [7]).

Since all parameters of the LFEF can be expected to be pressure dependent, this rather complicated behaviour is not surprising. At this stage, we do not attempt a quantitative calculation, mainly since the parameters

$$C'_{34}\left[\frac{a}{2}\right] \chi_Q^2 \chi_F^2 \cos q_a a\,, \quad A_{11}\left[\frac{c}{2}\right] \rho_Q^2 \cos \frac{q_c c}{2}\,,$$

$$A_{22}\left[\frac{c}{2}\right] \rho_F^2 \cos \frac{q_c c}{2}$$

have not yet been calculated, and they seem to be essential for a quantitative calculation. However, we can point out at this stage that a particularly strong pressure dependence is expected for A_{33} and A_{44} ($-$ d ln A_{33}/d ln $b \approx 21$ for a Lennard Jones potential [47]). The pressure variation of A_{44} is expected to be even stronger, since the TTF η-libration at 40 cm^{-1} is particulary soft. This frequency is determined from the Debye-Waller factor [22], which shows also that the analogous mode in TCNQ is much harder ($\sim$ 60 cm^{-1}). Raman effect measurements by Kuzmany and Stoltz [48] verify the presence of modes at these frequencies in TTF-TCNQ. Measurements of the Bordeaux group show that in the analogous compounds TTTF-TCNQ [49], HMTTF-TCNQ [50] and HMTSF-TCNQ [51], the donor η-libration is much harder ($\sim$ 60 cm^{-1}).

Also, $A_{12}[a/2]$ is expected to increase rapidly with pressure, because of the change in charge transfer [52], and the vanishing of this term for a charge transfer of approximately 0.5. Thus, at 20 kbar, where the charge transfer increases from 0.59 to 0.66 [45], $A_{12}[a/2]$ may increase by a factor of 2 or so, while A_{14}^2/A_{44}, A_{23}^2/A_{33} may be expected to decrease by a factor of 2 or so. $A_{11}[a]$ and $A_{22}[a]$ should be much less affected, since they do not depend critically upon the charge transfer. Since the 2 a period, and the existence of two separate phase transitions, depend on A_{14}^2/A_{44} to overwhelm A_{12}, this condition no longer exists above 15 kbar, and therefore, only one transition (possible with $q_a = 0$) should be present in agreement with experiment. According to our previous discussion it is plausible that the transition from the $q_a = \pi/a$, separate T_{p1} and T_{p2} state, proceeds *via* two Lifschitz points. However, a quantitative calculation has yet to be carried out. The commensurability term proposed by Friend *et al.* [45], increasing T_{p1} and giving rise to a first order transition there, must also be included.

7. **Discussion.** — We have shown here that because of the large number of parameters in the LFEF, symmetry considerations alone are not sufficient to determine the phase transitions since virtually an infinite range of possibilities exists. Therefore, *ab-initio* calculations of the parameters of the LFEF are essential for an understanding of the phase transitions of TTF-TCNQ.

We demonstrated that there is ground to believe that Coulomb coupling between CDW's cannot account for the two successive transitions at 48 K and 53 K, while the CDW-libron coupling accounts immediately for the existence of the two separate transitions, and the temperature dependence of the transverse period.

The crucial point in the CDW-libron model is the existence of the libron order parameters χ. Our estimations give for $T \sim 38$ K, $\chi_F \simeq 0.34$ deg. and $\chi_Q \approx 0.17$ deg. The question arises about the experimental evidence for such rotations. We note that in the TTF_5-I_7 salt Johnson and Watson [37] detected rotations with an amplitude of the order of $\chi \sim 5^o$. The reason why in the scattering experiments up to date these rotations were not detected lies partially in the smaller value of χ in TTF-TCNQ in comparison with TTF_7-I_5, also the measurements on TTF_7-I_5 involved intensity measurements of a few thousand Bragg spots; no such detailed work has been done on TTF-TCNQ. The careful search for the libron order parameter in TTF-TCNQ is very desirable.

The CDW-libron model predicts various possible phases; one disordered phase, and four ordered phases : $\rho_Q\,\chi_F$; $\rho_F\,\chi_Q$; $\rho_Q\,\chi_F\,\rho_P\,\chi_F$; ρ_F, ρ_Q, $\chi_F = \chi_Q = 0$. The realization of these phases depends upon the values of the LFEF parameters. It is interesting to note that it is possible to influence these parameters not only by external pressure but also by chemical substitutions (i.e. replacing S by Se).

The TTF-TCNQ system may be an appropriate system for the realization of the Lifshitz point. This is interesting because the critical behaviour near this point is peculiar.

We note also the interesting behaviour of C_p near the second phase transition (see Fig. 5). The maximum of the $C_p(T)$ curve is due to the A_{12}-interaction. Its realization is due to the closeness of the two successive phase transitions. This $C_p(T)$ behaviour exists also in the frame of the CDI model.

We developed here a method for estimating the various interaction parameters. This method may be easily generalized for more realistic wave functions of a TCNQ(TTF) molecule.

The present work is a first step of an *ab-initio* calculation of the phase transitions in TTF-TCNQ and analogous systems. Further work must include :

1) Calculation of the interaction parameters in the c^*-direction, and perhaps the [101] direction [19, 53] ([1]).

2) Calculation of fourth-order terms; in particular, the term $C'_{34}\,\chi_Q^2\,\chi_F^2$ which is responsible for the first order transition at 38 K, the locking to the 4 a period, and the peculiar properties of the state below 38 K.

3) Calculations of the interaction parameters in more realistic models to account for various screening effects, polarizability of molecules, etc.

4) The redistribution in charge of the molecules brought about by the translations and rotations. This redistribution changes the electron-phonon coupling constants considerably. Also, non-rigid distortions (intra-molecular phonons) must be considered.

5) The variation of the various parameters with volume, that should account for the rather complicated phase diagram observed.

6) The microscopic theory of the Peierls transi-

([1]) Recent calculations show that the interaction between similar chains in the c^* direction is strong ($a_{11}(c/2)$, $a_{22}(c/2) \sim 50$ meV). This interaction should be responsible for the decreasing of the fluctuations and the restoring of the mean field transition temperature.

tion, for the case when several phonons go soft simultaneously.

7) The effect of electron hopping between the chains on the various parameters.

8) The effect of the finite lifetime of the electronic states on the various parameters.

APPENDIX I

Calculation of the A_{14} interaction parameter. — The one electron tight-binding TCNQ chain wave function

$$\Psi_{\mathbf{k}}(\mathbf{r}) = \frac{1}{\sqrt{N}} \sum_n \varphi(\mathbf{r} - \mathbf{R}_n)\, e^{i\mathbf{k}.\mathbf{R}_n} \qquad (A.1)$$

is built of the molecular wave function which we approximate by the LCAO w.f.

$$\varphi(\mathbf{r} - \mathbf{R}_n) = \sum_i c_i\, \psi_i(\mathbf{r} - \mathbf{R}_{ni}) \qquad (A.2)$$

where $\psi_i(\mathbf{r} - \mathbf{R}_{ni})$ is the atomic wave function of atom i belonging to the n-th TCNQ molecule.

Substituting eq. (A.1) and (A.2) into eq. (25) we get

$$M_{14}(\mathbf{q}) = \sum_n e^{i\mathbf{q}\mathbf{R}_n} \sum_i |c_i|^2 \times$$
$$\times e \int \psi_i^*(\mathbf{r} - \mathbf{R}_{ni}) \frac{\partial V(\mathbf{r})}{\partial \chi_F}\bigg|_{\chi_F = 0} \psi_i(\mathbf{r} - \mathbf{R}_{ni})\, d^3 r \qquad (A.3)$$

where $\frac{\partial V(r)}{\partial \chi_F} \delta\chi_F$ is the potential change due to a libration $\delta\chi_F$ of one $TTF^{+0.6}$ molecule. When the net charge distribution on the $TTF^{+0.6}$ molecule is taken in the form $e \sum_j z_j\, \delta(\mathbf{r} - \mathbf{R}_j)$ we obtain

$$\frac{\partial V_i}{\partial \chi_F}\bigg|_{\chi_F = 0} = \sum_j e z_j \frac{\partial R_{ij}^{-1}}{\partial \chi_F}\bigg|_{\chi_F = 0} \qquad (A.4)$$

where z_j is the net charge (in units of the electron charge e) of the j-th atom of the $TTF^{+0.6}$ molecule and R_{ij} is the distance between the i and j atoms. If we neglect the spread of the charge around the atoms ($\psi_i(\mathbf{r} - \mathbf{R}_{ni}) \approx \delta(\mathbf{r} - \mathbf{R}_{ni})$) then

$$M_{14}(\mathbf{q}) = \sum_n e^{i\mathbf{q}.\mathbf{R}_n} \sum_{ij} |c_i|^2 z_j e^2 \frac{\partial R_{ij}^{-1}(n)}{\partial \chi_F}\bigg|_{\chi_F = 0}. \qquad (A.5)$$

The summation over n can be broken into four summations over the four bridges shown in figure 12. For the first bridge (see Fig. 12)

$$\frac{\partial R_{ij}^{-1}}{\partial \chi_F}\bigg|_{\chi_F = 0} =$$
$$= R_{ij}^{-3}(\Delta x\, \zeta_j^0 + \Delta y \sin \theta_F\, \xi_j^0 + \Delta z \cos \theta_F\, \xi_j^0) \qquad (A.6)$$

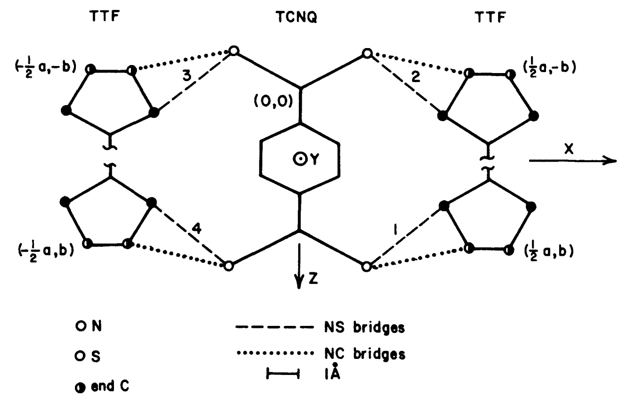

Fig. 12. — The interaction bridges for the nearest neighbours chains.

where

$$\begin{aligned} R_{ij}^2 &= (\Delta x)^2 + (\Delta y)^2 + (\Delta z)^2 \\ \Delta x &= \xi_j^0 + \frac{a}{2} - \xi_i^0 \\ \Delta y &= (p + \varepsilon)\, b\,; \quad p = 0, \pm 1, \pm 2, \ldots \\ b\varepsilon &= -\zeta_i^0 \sin \theta_Q - \zeta_j^0 \sin \theta_F \\ \Delta z &= \zeta_i^0 \cos \theta_Q - \zeta_j^0 \cos \theta_F \end{aligned} \qquad (A.7)$$

where ξ^0, η^0, ζ^0 are the coordinates of the corresponding atom in the coordinate system of the mole-

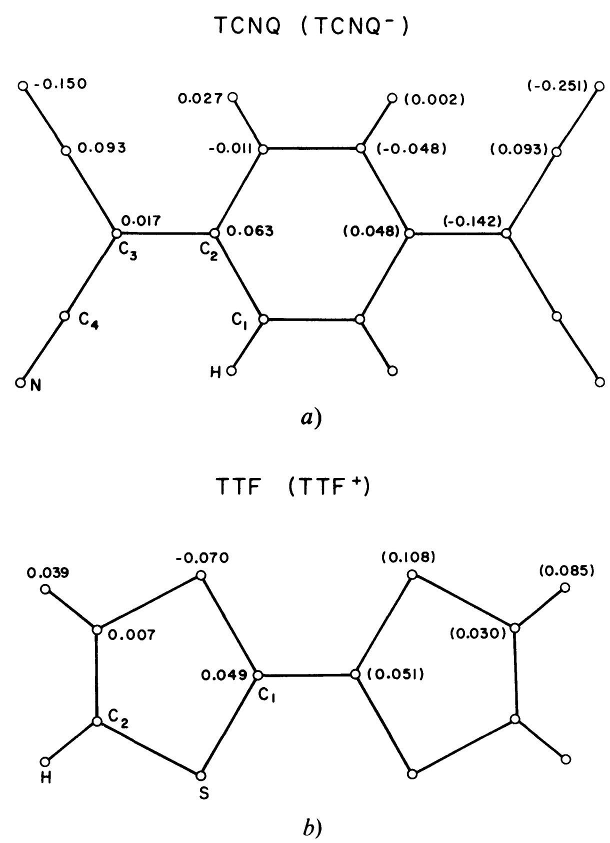

Fig. 13. — Net charge on each atom of the TTF(TTF^+) and TCNQ($TCNQ^-$) from reference [25]. These values were used in the calculations of the charge densities listed in table II.

cule (see Fig. 1*b*). For the other three bridges we obtain

$$\begin{array}{lll} \Delta x_2 = \Delta x & \varepsilon_2 = -\varepsilon & \Delta z_2 = -\Delta z \\ \Delta x_3 = -\Delta x & \varepsilon_3 = -\varepsilon & \Delta z_3 = -\Delta z \\ \Delta x_4 = -\Delta x & \varepsilon_4 = \varepsilon & \Delta z_4 = \Delta z . \end{array} \quad (A.8)$$

Performing in eq. (A.5) the summation over the four interaction bridges we obtain

$$M_{14}(\mathbf{q}) = 4 \sin\left(q_a \frac{a}{2}\right) \sum_{p=-\infty}^{\infty} \sin\left(\frac{2\pi b}{\Lambda} p\right) \times \times \sum_{ij} |c_i|^2 z_j e^2 \frac{\partial R_{ij}^{-1}}{\partial \chi_F} . \quad (A.9)$$

The nearest neighbour approximation is obtained when only $p = 1$ is taken (the $p = 0$ contribution is zero because of the symmetry of the configuration as can be seen in eq. (A.9)). To perform the summation in eq. (A.9) we write the derivatives from eq. (A.6) in the form (for simplicity, we omit the indices i, j)

$$\left.\frac{\partial R^{-1}}{\partial \chi_F}\right|_{\chi_F = 0} = \frac{A + B(p+\varepsilon) b}{[d_\perp^2 + (p+\varepsilon)^2 b^2]^{3/2}} \quad (A.10)$$

where

$$\begin{aligned} A &= \Delta x \, \zeta_j^0 + \Delta z \cos \theta_F \, \xi_j^0 \\ B &= \sin \theta_F \, \xi_j^0 \\ d_\perp^2 &= (\Delta x)^2 + (\Delta z)^2 \end{aligned} \quad (A.11)$$

and use the integral representation

$$[d_\perp^2 + (p+\varepsilon)^2 b^2]^{-\frac{2n+1}{2}} = \frac{2}{\pi} \frac{1}{(2n-1)!!} \int_0^\infty \cos[ub(p+\varepsilon)] \frac{K_n(ud_\perp)}{d_\perp^n} u^n \, du \quad (A.12)$$

$$n = 0, 1, 2, \ldots$$

where $K_n(x)$ is the modified Bessel function of the n-th order with the asymptotic behaviour

$$K_n(x) \approx \sqrt{\frac{\pi}{2x}} e^{-x} .$$

For $n = 0$ this representation was used by Saub, Barisic and Friedel [54]. After some calculations we obtain from eq. (A.10) and eq. (A.12) that

$$\sum_{p=-\infty}^{\infty} \frac{\partial R^{-1}}{\partial \chi_F} \sin(q_b pb) = \frac{2}{b} \left\{ -A \sum_{n=-\infty}^{\infty} |q_b + g_n| \frac{K_1(|q_b + g_n| d_\perp)}{d_\perp} \sin[(q_b + g_n) b\varepsilon] + \right. \\ \left. + B \sum_{n=-\infty}^{\infty} (q_b + g_n) K_0(|q_b + g_n| d_\perp) \cos[(q_b + g_n) b\varepsilon] \right. \quad (A.13)$$

where $g_n = \frac{2\pi}{b} n$ is a reciprocal lattice vector. The substitution of (A.13) into eq. (A.9) gives the final result for the $M_{14}(\mathbf{q})$ matrix element. The series converges very fast, and two terms are sufficient. The geometrical factors, A, B, $d_\perp$ and ε depends upon the tilting angles and coordinates ξ^0, η^0, ζ^0 of corresponding atoms.

In the second model where all the pair interactions between atoms of the TTF and TCNQ molecules are taken into account in the summation of eq. (A.5), a total of 20 × 14 pair interactions must be calculated. All of these calculations were performed with the help of the computer.

APPENDIX II

A. **Calculation of the A_{12}-parameter.** — 1. The contribution to A_{12} from the interference effect is obtained from eq. (31). The calculation of this contribution is the same as in the previous case of the A_{14}-parameter. Instead of $\partial R_{ij}^{-1}/\partial \chi_F$ now appears the derivative $\partial R_{ij}^{-1}/\partial \rho$. The latter has the same form as eq. (A.10), only the parameters A and B of eq. (A.10) will be different. The results of calculation are given in table IV. Some matrix elements calculated in the NN approximation are listed in table III.

2. The CDW-CDW contribution to the A_{12} parameter is the sum of the Coulomb interaction between corresponding pairs of CDW's on the TCNQ and TTF stacks. The charge distribution in a chain is supposed to be

$$\rho^{(0)}(\mathbf{r}) = \sum_{in} e \, |c_i|^2 \, \nu \, \delta(\mathbf{r} - \mathbf{R}_{ni}) \quad (A.14)$$

where c_i is the LCAO coefficient of the molecular wave function, ν is the charge transfer ($\nu \approx 0.6$) and $\mathbf{R}_{ni}$ is the position of the i-th atom in the n-th molecule. In the presence of a CDW this charge distribution is modulated :

$$\rho(\mathbf{r}) = \sum_{in} e \, |c_i|^2 \, \nu \, \delta(\mathbf{r} - \mathbf{R}_{ni}) \left[1 + \kappa \cos(q_b nb + \varphi)\right] . \quad (A.15)$$

Eq. (A.15) defines the discrete CDW model with the assumption that the amplitude κ and the phase φ is the same for each atom of the molecule. This equation defines κ as the CDW amplitude relative to the average charge transfer. The CDW-CDW interaction energy per cell is equal to

$$E_{12} = v^2 e^2 \kappa_Q \kappa_F \sum_{ij} | c_i |^2 | c_j |^2 \frac{1}{2N} \sum_{n,m=-N}^{N} \frac{\cos(q_b nb + \varphi_1) \cos(q_b mb + \varphi_2)}{R_{ij}(n-m)} =$$

$$= v^2 e^2 \kappa_Q \kappa_F \sum_{ij} | c_i |^2 | c_j |^2 \frac{1}{2} \sum_{p=-\infty}^{\infty} \frac{\cos(q_b pb + \varphi_{12})}{R_{ij}(p)} . \quad (A.16)$$

Using eq. (A.12) for $n = 0$ we transform eq. (A.16) into a sum over the reciprocal lattice wave numbers [54]. After summation over four interaction bridges, we obtain in full analogy with the above described A_{14} calculation that the CDW-CDW interaction energy per (cell) between neighbouring TCNQ and TTF stacks is equal to :

$$E_{12} = 2 a_{12} \cos \varphi_{12} \cos \left(\frac{q_a a}{2} \right) \kappa_Q \kappa_F \quad (A.17)$$

where

$$a_{12} = \frac{2 e^2 v^2}{b} \sum_{ij} | c_i |^2 | c_j |^2 \sum_{n=-\infty}^{\infty} \cos [(q_b + g_n) b\varepsilon_{ij}] K_0(| q_b + g_n | d_{\perp ij}) \quad (A.18)$$

$\cos \varphi_{12} = -1$ in eq. (A.17) according to the minimum conditions for the free energy.

The first ($g_n = 0$) term in eq. (A.18) gives the quasi continous CDW approximation where the discrete stacks of molecules are replaced by continuous threads passing through each atom of the molecules. Additional terms contribute about 25 % of the total value depending on the value of $d_\perp$. For $d \geqslant 6$ Å terms other than the first can be neglected.

B. Calculation of the next nearest neighbour interaction parameters. — The CDW-CDW interaction between similar chains was calculated in the same manner as in the NN CDW-CDW interaction. For example, the TCNQ-TCNQ interaction is

$$a_{11}(a) = \frac{4 e^2 v^2}{b} \sum_{ij} | c_i |^2 | c_j |^2 \cos (q_b b\varepsilon_{ij}) K_0(q_b d_{\perp ij}) \quad (A.19)$$

where i and j refer to atoms in a pair of neighbouring TCNQ stacks. Terms with g_n other than zero were neglected due to the large distances between similar chains. The values of a_{12}, $a_{11}(a)$ and $a_{22}(a)$ are listed in table V.

References

[1] FERRARIS, J. P., COWAN, D. O., WALATKA, V. V., PERLSTEIN, J. E., *J. Am. Chem. Soc.* **95** (1973) 948.

[2] HEEGER, A. J. and GARITO, A. F., in *Low Dimensional Cooperative Phenomena*, J. J. Keller Ed. (Plenum Press) 1974.

[3] CRAVEN, R. A., SALAMON, M. B., DEPASQUALI, G., HERMAN, R. M., STUCKY, G., SCHULTZ, A., *Phys. Rev. Lett.* **32** (1974) 769.

[4] COMES, R., SHIRANE, G., SHAPIRO, S. M., GARITO, A. F., HEEGER, A. J., *Phys. Rev.* **14** (1976) 2376.

[5] RYBACZEWSKI, E. F., SMITH, L. S., GARITO, A. F., HEEGER, A. J., SILBERNAGEL, B. G., *Phys. Rev.* **B 14** (1976) 2746.

[6] ETEMAD, S., *Phys. Rev.* **B 13** (1976) 2254.

[7] COOPER, J. R., JEROME, D., WEGER, M., ETEMAD, S., *J. Physique Lett.* **36** (1975) L-219.

[8] JEROME, D., MULLER, W., WEGER, M., *J. Physique Lett.* **35** (1974) L-77.

[9] *Chemistry and Physics of One-Dimensional Metals*, H. J. Keller Ed. (Plenum Press) 1977.

[10] *Organic Conductors and Semiconductors*, Conference Proceedings, Siofok, Hungary, 1976. *Lecture Notes in Physics* **65** (Springer Verlag) 1977.

[11] ETEMAD, S., ENGLER, E. M., SCHULTZ, T. D., PENNEY, T., SCOTT, B. A., *Phys. Rev.* **B 17** (1978) 513.

[12] COMES, R., SHAPIRO, S. M., SHIRANE, G., GARITO, A. F., HEEGER, A. J., *Phys. Rev. Lett.* **35** (1975) 1518.

[13] BAK, P., EMERY, V., *Phys. Rev. Lett.* **36** (1976) 978.

[14] SCHULTZ, T. D., ETEMAD, S., *Phys. Rev.* **B 13** (1976) 4928.

[15] BJELIS, A., BARISIC, S., in *Organic Conductors and Semiconductors*, Conference Proceedings, Siofok, Hungary, 1976. *Lecture Notes in Physics* **65** (Springer Verlag) 1977, p. 291.

[16] ABRAHAMS, E., SOLYOM, J., WOYNAROVICH, F., *Phys. Rev.* **B 16** (1977) 5238.
ABRAHAMS, E., DZYALOSHINSKII, I. E., *Solid State Commun.* **23** (1977) 883.

[17] SY, H. K., MAVROYANNIS, C., *Solid State Commun.* **23** (1977) 79.

[18] MUKAMEL, D., *Phys. Rev.* **B 16** (1977) 1741.

[19] HOROVITZ, B., MUKAMEL, D., *Solid State Commun.* **23** (1977) 285.

[20] MORAWITZ, H., *Phys. Rev. Lett.* **34** (1975) 1096.
MERIFIELD, R. E., SUNA, A., *Phys. Rev. Lett.* **36** (1976) 826.
MORAWITZ, H. in ref. [10], page 303.

[21] WEGER, M., FRIEDEL, J., *J. Physique* **38** (1977) 241 and *ibid.* **38** (1977) 881.

[22] SCHULTZ, A. J., STUCKY, G. D., BLESSING, R. H., COPPENS, P., *J. Am. Chem. Soc.* **98** (1976) 3194.

[23] WEGER, M. and GUTFREUND, H., *Comments Solid State Phys.* **8** (1978) 135.
GUTFREUND, H., KAVEH, M. and WEGER, M., *Quasi-One-Dimensional Conductors*, Conference Proceedings, Dubrovnik, Yugoslavia, 1978, *Lecture Notes in Physics* **95** (Springer Verlag) 1979, p. 105.
WEGER, M., *Proceedings NATO ASI*, Tomar, August 1979 (Plenum Press, New York) in press.

[24] HARTZSTEIN, C., ZEVIN, V., WEGER, M., *Quasi-One-Dimensional Conductors*, Conference Proceedings, Dubrovnik, Yugoslavia, 1978, *Lecture Notes in Physics* **95** (Springer Verlag) 1979, p. 76.

[25] LADIK, J., KARPFEN, A., STOLLHOFF, G., FULDE, P., *Chem. Phys.* **7** (1975) 267 and **8** (1975) 215.

[26] HORNREICH, R. M., LUBAN, M., SHTRIKMAN, S., *Phys. Rev. Lett.* **35** (1975) 1678, *Phys. Lett.* **A 55** (1975) 269, and to be published.

[27] WEGER, M., GOLDBERG, I. B., *Solid State Phys.* (ed. Seitz, Turnbull, Ehrenreich) **28** (1973) 1-177.

[28] FASOL, G., Ph. D. Thesis, Universitat Bochum (1978) unpublished.

[29] CHU, C. W., TESTARDI, L. R., *Phys. Rev. Lett.* **32** (1974) 766.

[30] FRIEDEL, J., *J. Physique Lett.* **36** (1975) L-279 and references therein.

[31] BYCHKOV, Y. A., GORKOV, L. O., DZYALOSHINSKII, I. E., *JETP* **23** (1966) 489.

[32] PEIERLS, R. E., *Quantum Theory of Solids* (Clarendon Press, Oxford) 1955.

[33] FROHLICH, H., *Proc. R. Soc.* **A 223** (1954) 296.

[34] KUPER, C. G., *Proc. R. Soc.* **A 227** (1955) 214.

[35] GUTFREUND, H., HOROVITZ, B., WEGER, M., *J. Phys.* **C 7** (1974) 383.

[36] COMES, R., in *Chemistry and Physics of One-Dimensional Metals*, ed. H. J. Keller NATO Advanced Study Institutes Series, Series V, Vol. **25** (Plenum Press, New York) 1977, p. 315.

[37] JOHNSON, C. K., WATSON, C. R., *J. Chem. Phys.* **64** (1976) 2271.

[38] DJUREK, D., FRANULOVIC, K., PRESTER, M., TOMIC, S., GIRAL, L., FABRE, J. M., *Phys. Rev. Lett.* **38** (1977) 715.

[39] ALLENDER, D., BRAY, J. W., BARDEEN, J., *Phys. Rev.* **B 9** (1974) 119.

[40] RICE, M. J., STRASSLER, S., *Solid State Commun.* **13** (1973) 125.

[41] NIELSEN, J., CARNEIRO, K., *Quasi-One-Dimensional Conductors*, Conference Proceedings, Dubrovnik, Yugoslavia, 1978, *Lecture Notes in Physics* **95** (Springer Verlag) 1979, p. 238.

[42] DIETRICH, W. and FULDE, P., *Z. Phys.* **265** (1973) 239.

[43] It may be shown that the coefficients of the $\rho_Q \chi_Q$ and $\rho_F \chi_F$ terms which follow from the interference effect is zero in agreement with symmetry considerations discussed in ref. [21].

[44] DEIGEN, M., ZEVIN, V., *JETP* **39** (1960) 1126 (*Sov. Phys. JETP* (1961) 785).
BARISIC, S., *Phys. Rev.* **B 5** (1972) 941 and references therein.
KONDO, J. and ANZAI, H., private communication.

[45] FRIEND, R. H., MILJAK, M., JEROME, D., *Phys. Rev. Lett.* **40** (1978) 1048.

[46] LANDAU, L., LIFCHITZ, E., *Statistical Physics* (Pergamon Press).

[47] GUTFREUND, H., WEGER, M., KAVEH, M., *Solid State Commun.* **26** (1978).

[48] KUZMANY, H. and STOLTZ, H. J., *J. Phys. C* **10** (1977) 2241.

[49] CHASSEAU, D., GAULTIER, J., HAUW, C., FABRE, J. M., GIRAL, L., TORREILL, E., *Acta Crystallogr.* **B 34** (1978) 2811.

[50] CHASSEAU, D., COMBERTON, G., GAULTIER, J. and HAUW, C., *Acta Crystallogr.* **B 34** (1978) 689, and private communication.

[51] GAULTIER, J., private communication.

[52] TIEDJE, T., HAERING, R. R., JERICHO, M. H., ROGER, W. A., SIMPSON, A., *Solid State Commun.* **23** (1977) 713.

[53] SHITZKOVSKY, S., WEGER, M., GUTFREUND, H., *J. Physique* **39** (1978) 711.

[54] SAUB, K., BARISIC, S., FRIEDEL, J., *Phys. Lett.* **56A** (1976) 302.

[55] SHIRANE, G., SHAPIRO, S. M., COMES, R., GARITO, A. F., HEEGER, A. J., *Phys. Rev.* **B 14** (1976) 2325.

[56] KISTENMACHER, T. J., PHILLIPS, T. E., COWAN, D. O., *Acta Crystallogr.* **B 30** (1974) 763.

[57] BRIGHT, A. A., GARITO, A. F., HEEGER, A. J., *Phys. Rev.* **B 10** (1974) 1328.
SALAHUB, D. R., MESSMER, R. D., HERMAN, F., *Phys. Rev.* **B 13** (1976) 5252.
TOMKIEVICH, Y., SCOTT, B. A., TAO., L. J., TITLE, R. S., *Phys. Rev. Lett.* **32** (1974) 1363.

[58] ELLENSON, W. D., COMES, R., SHAPIRO, S. M., SHIRANE, G., GARITO, A. F., HEEGER, A. J., *Solid State Commun.* **20** (1976) 53.
ELLENSON, W. D., SHAPIRO, S. M., SHIRANE, G., GARITO, A. F., *Phys. Rev.* **B 16** (1977) 3244.